9. Gysels M, Richardson A, Higginson IJ. Communication training for health professionals who care for patients with cancer: a systematic review of training methods. *Support Care Cancer.* 2005;13:356-366.
10. Gysels M, Richardson A, Higginson IJ. Communication training for health professionals who care for patients with cancer: a systematic review of effectiveness. *Support Care Cancer.* 2004;12:692-700.
11. Merckaert I, Libert Y, Razavi D. Communication skills training in cancer care: where are we and where are we going? *Curr Opinion Oncol.* 2005;17:319-330.
12. Fallowfield L, Jenkins V. Current concepts of communication skills training in oncology. *Recent Results Cancer Res.* 2006;168:105-112.
13. Baile WF, Kudelka AP, Beale EA, et al. Communication skills training in oncology. Description and preliminary outcomes of workshops on breaking bad news and managing patient reactions to illness. *Cancer.* 1999;86:887-897.
14. Baile WF, Buckman R, Renzi R, et al. SPIKES-A 6-step protocol for delivering bad news: application to the patient with cancer. *Oncologist.* 2000;5:302-311.
15. Fujimori M, Oba A, Koike M, et al. Communication skills training for Japanese oncologists on how to break bad news. J Cancer Educ. 2003;18:194-201.
16. Zigmond AS, Snaith RP. The hospital anxiety and depression scale. *Acta Psychiatr Scand.* 1983;67:361-370.
17. Kugaya A, Akechi T, Okuyama T, et al. Screening for psychological distress in Japanese cancer patients. *Jpn J Clin Oncol.* 1998;28:333-338.
18. Kitamura T. Hospital anxiety and depression scale [in Japanese]. *Seishinka Sindangaku.* 1993;4:371-372.
19. Watson M, Greer S, Young J, et al. Development of a questionnaire measure of adjustment to cancer: the MAC scale. *Psychol Med.* 1998;18:203-209.
20. Watson M, Greer S, Bliss JM. Mental Adjustment to Cancer scale user's manual. London, UK: Royal Marsden Hospital; 1989.
21. Akechi T, Kugaya A, Okamura H, et al. Validity and reliability of the Japanese version of the Mental Adjustment to Cancer (MAC) scale [in Japanese]. *Jpn J Psychiatr Treat.* 1997;12:1065-1071.
22. Umezawa S, Fujimori M, Uchitomi Y. Care for patients who were informed of bad news [in Japanese]. *Jpn J Cancer Care.* 2006;11:767-770.
23. Fallowfield L, Jenkins V, Farewell V, Saul J, Duffy A, Eves R. Efficacy of a Cancer Research UK communication skills training model for oncologists: a randomised controlled trial. *Lancet.* 2002;359:650-656.
24. Fallowfield L, Jenkins V. Communicating sad, bad, and difficult news in medicine. *Lancet.* 2004;363:312-319.
25. Razavi D, Merckaert I, Marchal S, et al. How to optimize physicians' communication skills in cancer care: results of a randomized study assessing the usefulness of posttraining consolidation workshops. *J Clin Oncol.* 2003;21:3141-3149.
26. Baile WF, Buckman R, Schapira L, et al. Breaking bad news: more than just guidelines. *J Clin Oncol.* 2006;24:3217; author reply 3217-3218.
27. Singer MK, Wellish DK, Durvasula R. Impact of breast cancer on Asian American and Anglo American women. *Culture Med and Psychiatr.* 1997;21:449-480.
28. Uchitomi Y, Sugihara J, Fukue M, et al. Psychiatric liaison issues in cancer care in Japan. *J Pain Symptom Manage.* 2004;9:319-324.
29. Lomas D, Timmins J, Harley B, et al. The development of best practice in breaking bad news to patients. *Nurs Times.* 2004;100:28-30.

Abnormal Expression of $p16^{INK4a}$, Cyclin D1, Cyclin-Dependent Kinase 4 and Retinoblastoma Protein in Gastric Carcinomas

ICHIRO KISHIMOTO, MD,[1] HIROYUKI MITOMI, MD,[2]* YASUO OHKURA, MD,[3] HIDEKI KANAZAWA, MD,[1] NAOSHI FUKUI, MD,[4] AND MASAHIKO WATANABE, MD[5]

[1]Department of Surgery, National Hospital Organization Sagamihara Hospital, Kanagawa, Japan
[2]Department of Clinical Research Laboratory (Pathology Division), National Hospital Organization Sagamihara Hospital, Kanagawa, Japan
[3]Department of Pathology, Kyorin University School of Medicine, Tokyo, Japan
[4]Department of Pathomechanisms, Clinical Research Center, National Hospital Organization Sagamihara Hospital, Kanagawa, Japan
[5]Department of Surgery, School of Medicine, Kitasato University, Kanagawa, Japan

Background and Objectives: The $p16^{INK4a}$ (p16), cyclin D1, cyclin-dependent kinase (CDK) 4 and retinoblastoma (Rb) genes are components of the Rb pathway that controls the G1-S checkpoint of the cell cycle. The aim of this study was to assess the relationship between their abnormalities and clinicopathological features in gastric carcinomas.
Mehtods: Immunohistochemical analysis of the encoded proteins was performed on a series of 158 cases.
Results: Loss of p16/Rb protein (pRb) expression and overexpression of cyclin D1/CDK4 were observed in 49%/40% and 37%/37% of gastric carcinomas, respectively. At least 1 of these abnormalities was found in 86% of the cases and a positive correlation was noted between p16 and pRb ($P = 0.009$). Cyclin D1 ($P = 0.042$) and CDK4 ($P = 0.008$) overexpession was inversely associated with lymph node metastasis and depth of invasion, respectively. Loss of pRb expression was more frequently in diffuse type lesions than in the intestinal type ($P = 0.022$). The patients with p16+/pRb−/cyclin D1−/CDK4− or p16−/pRb+/cyclin D1−/CDK4− tumors demonstrated particularly poor survival. With multivariate survival analysis, only depth of invasion and TNM stage could be proven as independent predictors.
Conclusions: The Rb pathway is disrupted in the vast majority of gastric carcinomas. This study also identified specific immunohistochemical marker profiles for prognosis.
J. Surg. Oncol. © 2008 Wiley-Liss, Inc.

KEY WORDS: **gastric carcinoma; $p16^{INK4a}$; retinoblastoma protein; cyclin D1; CDK4; prognosis**

INTRODUCTION

In the normal situation, cell proliferation appears to be regulated by several different cascades of molecules, many of which are known to be oncogene products or tumor-suppressor proteins. In the development of neoplasia, loss of this cell cycle control is a critical step. The late G1 cell cycle checkpoint is controlled by a complex of proteins, which includes $p16^{INK4a}$ (p16), cyclin D1, cyclin-dependent kinase (CDK) 4/6, and retinoblastoma protein (pRb) [1]. They are components of the pRb cell cycle control pathway; cyclin D1 stimulates phosphorylation of pRb by associating with CDKs [2] and p16 binds to CDK4/6, blocking their association with D-type cyclins [1]. Thus, loss of p16 or pRb expression, or overexpression of cyclin D1 or CDK4/6 cause pRb pathway dysfunction and stimulate cell proliferation. For this reason, it is better to analyze all four of these genes together rather than study them individually. However, there have been few studies of patterns and prognostic value of their expression in gastric carcinomas [3,4]. The present study was thus undertaken to determine the disturbance in the pRb pathway with expression of these four related genes in gastric carcinomas and to explore their correlation with clinicopathological features and prognosis.

MATERIALS AND METHODS

Patients and Materials

The subjects of the present study comprised a series of 158 patients diagnosed and undergoing potentially curative surgery for gastric carcinoma at the National Hospital Organization Sagamihara Hospital between August 1999 and June 2006. The 158 patients comprised 108 males and 50 females, with a mean age of 66.5 years (range, 36–91). Patients with multiple gastric carcinomas or with distant metastasis, and patients who had died within 30 days of surgery were not included in the analysis. No patient received initial chemotherapy or radiotherapy and standard informed consent was obtained in all cases.

Pathological Review

Surgically resected specimens had been fixed in 10% formalin and embedded in paraffin wax, according to routine procedures. Slides stained with hematoxylin and eosin were examined by an experienced gastrointestinal pathologist (H.M.). Curative surgery was finally defined as the removal of all gross tumors and the demonstration of tumor-negative surgical margins by microscopic examination of the total circumference of the resection line. The histological type was classified as intestinal or diffuse according to the criteria of Laurén [5].

I. Kishimoto and H. Mitomi contributed equally to this study.

Grant sponsor: Parents' Association Grant (Keyaki-kai) of Kitasato University, School of Medicine.

*Correspondence to: Hiroyuki Mitomi, MD, Department of Clinical Research Laboratory (Pathology Division), National Hospital Organization Sagamihara Hospital, 18-1 Sakura-dai, Sagamihara, Kanagawa 228-8522, Japan. Fax: 81-42-742-5314. E-mail: h-mitomi@sagamihara-hosp.gr.jp

Received 26 November 2007; Accepted 15 April 2008
DOI 10.1002/jso.21087
Published online in Wiley InterScience(www.interscience.wiley.com).

The depth of invasion (pT category), lymph node involvement (pN category) and pathological staging, of all surgically resected tumors was completed according to the UICC/TNM classification [6]. Of the total, 98 were diagnosed pathologically as TNM stage I, 29 as stage II, 22 as stage III and 9 as stage IV.

Follow-up

All patients were followed up regularly by clinical examination at 1- to 2-month intervals for the first year and 3- to 6-month intervals thereafter. They underwent routine physical and blood examinations including measurement of serum carcinoembryonic antigen levels, liver functions and complete blood cell counts. Endoscopy was performed perioperatively and every year thereafter. Screening with ultrasound, computed tomography or magnetic resonance imaging was also mandated at 3–6 monthly intervals for the first year and once a year thereafter. Overall survival (OS) was measured from the date of surgery to the end of follow-up or death due to gastric cancer or other causes. Recurrence-free survival (RFS) was defined as the time from surgery to recurrent disease (alive) or death. The mean duration of patients' follow-up was 43 months (median, 41 months; range, 12–103 months) for those who were alive at the date of their last visit (n = 117).

Immunohistochemistry

Methodology. Immunostaining was performed on 4 μm thick slides that were prepared from each tumor with DakoCytomation Autostainer Instruments (DakoCytomation, Kyoto, Japan). Briefly, the sections were deparaffinization in xylene and rehydrated in decreasing concentrations of ethanol. Endogeneous peroxidase activity was blocked by incubation with Peroxidase-Blocking Solution (Dako A/S Ltd., Glostrup, Denmark) for 5 min. Antigen retrieval was required for all antibodies and consisted of autoclave treatment of sections for 30 min in either Epitope Retrieval Solution (DakoCytomation) for p16 or Target Retrieval Solution (pH 6.0, DakoCytomation) for cyclin D1, CDK4 and pRb. The slides were then incubated with primary antibodies for 30 min at room temperature. Envision Kits (DakoCytomation) were employed; the slides were incubated with horseradish peroxidase-labeled polymer conjugated with secondary antibody for 30 min and incubated with Substrate-Chromogen (diaminobenzidine) Solution (DakoCytomation), followed by light counterstaining with Mayer's hematoxylin.

Antibodies. Antibodies employed were monoclonal anti-p16 (E6H4, prediluted, DakoCytomation), monoclonal anti-cyclin D1 (SP4, prediluted, Nichirei, Tokyo, Japan), polyclonal anti-CDK4 (C-22, 1:600, Santa Cruz Biotechnology, Inc., Santa Cruz, CA) and monoclonal anti-pRb (Rb1, 1:200, DakoCytomation).

Controls. Sections of a squamous cell carcinoma of the esophagus with known positivity for p16 and a thyroid papillary carcinoma with known positivity for cyclin D1, CDK4 and pRb were used as external positive controls. For negative controls, the primary antibodies were omitted.

Assessment of staining. Distinct nuclear staining for all antibodies was considered to be positive, regardless of the staining intensity. When there was cytoplasmic staining, a nucleus was regarded as positive if its staining intensity equaled or exceeded that of the surrounding cytoplasm. All sections were evaluated by one pathologist (H.M.) unaware of the disease outcome. For p16 and pRb, <5% expression (−) was considered as loss. For cyclin D1 and CDK4, ≥5% (+) was regarded overexpression. Loss of p16 and Rb expression (p16−/Rb−) and overexpression of cyclin D1 and CDK4 (cyclin D1+/CDK4+) was considered abnormal.

Statistical analysis

The chi-squared test (with Yates' correction) and Fisher's exact test were applied to check for associations between categorical data. Survival curves were generated by the Kaplan-Meier method. To identify survival differences (good, intermediate and poor prognosis groups), specific marker profiles of combined immunohistochemical results for the four genes were clustered using multiple cutoff points and were analyzed for survival rates with resultant hazard ratios and P values. Associations between clinicopathological features and survival were examined using univariate and multivariate Cox's regression analyses. For the Cox's multivariate analysis, a step-wise backward variable elimination method was used with an entry limit of $P < 0.1$ and a removal limit of $P \geq 0.05$. All P values <0.05 were considered statistically significant. Statistical analyses were carried out using StatView for Windows Version 5.0 (SAS Institute, Inc., Cary, NC).

RESULTS

p16, Cyclin D1, CDK4 and pRb Expressions in Gastric Mucosa

In few cases, very weak p16 reactivity was found in the neck zone of normal glands, and in some cases the antigen demonstrated relatively strong expression at the bottoms of the regenerative and metaplastic glands (Fig. 1A). In some cases, cyclin D1 was weakly expressed in the neck zone of normal glands and foveolar epithelial cells. In the non-neoplastic tissues, immunoreactivities of p16 and cyclin D1 were less than 5%. No expression of CDK4 was apparent in non-neoplastic mucosa. On the other hand, pRb was positive throughout the normal and regenerative epithelium with or without intestinal metaplasia, more than 50% of cells exhibiting clear staining (Fig. 1C).

Expression of the Encoded Proteins in Gastric Carcinomas

Basically, p16 and CDK4 showed nuclear/cytoplasmic staining, and cyclin D1 and pRb nuclear immunoreactivity for all staining, most carcinomas showed a mosaic pattern throughout the lesions. Of the 158 tumors, 77 (49%) and 63 (40%) demonstrated loss of expression for p16 (Fig. 1B) and pRb (Fig. 1D), respectively. Some of the tumors overexpressed cyclin D1 (58/158, 37%; Fig. 1E) and CDK4 (59/158, 37%; Fig. 1F), respectively.

Correlation Among Expression of the Encoded Proteins

Abnormal expression of at least 1 protein was apparent in 136 (86%) carcinomas. Expression of p16 was positively associated with pRb immunoreactivity, but no correlations were noted among the other parameters (Table I).

Associations With Clinicopathological Features

Cyclin D1 overexpression was more prevalent in node-negative than in node-positive cases. CDK4 overexpession was inversely related to the pT category. Loss of pRb expression was more frequent in the diffuse type of Laurén's classification than in the intestinal type. No significant relationship was observed between p16 expression and clinicopathological variables (Table II).

Survival

Clinicopathological features were analyzed by univariate analysis as risk factors for OS and RFS. Based on this analysis, tumor size, the

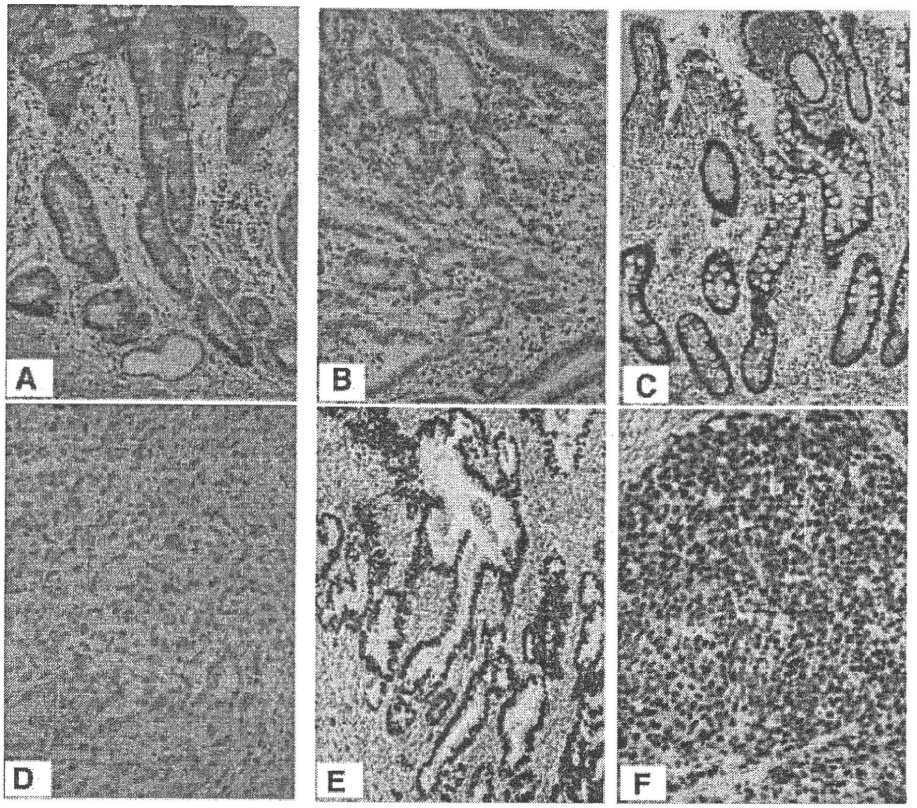

Fig. 1. **A**: p16 reactivity is focally apparent at the bottoms of non-neoplastic regenerative glands (original magnification 25×). **B**: Decreased expression of p16 in an intestinal type gastric adenocarcinoma (original magnification 30×). **C**: pRb is reactive throughout regenerative epithelium characterized by intestinal metaplasia (original magnification 18×). **D**: pRb demonstrates loss of nuclear immunoreactivity in a diffuse type adenocarcinoma (original magnification 34×). **E**: Strong nuclear staining of cyclin D1 in an intestinal type adenocarcinoma (original magnification 25×). **F**: CDK4 expression in the nuclei and cytoplasm of a diffuse type adenocarcinoma (original magnification 41×). [Color figure can be viewed in the online issue, available at www.interscience.wiley.com.]

pT category, the pN category and the TNM stage had a significant influence on OS and RFS (Table III).

Three distinct prognosis groups were identified: a good prognosis group with 10 patterns of marker profiles, and intermediate and poor prognosis groups with 4 and 2 patterns of marker profiles, respectively. Patients with p16+/pRb−/cyclin D1−/CDK4− or p16−/pRb+/cyclin D1−/CDK4− tumors demonstrated particularly poor survival whereas patients with p16+/pRb−/cyclin D1+/CDK4+, p16−/pRb+/cyclin D1−/CDK4+ or p16−/pRb−/cyclin D1−/CDK4+ tumors were all alive. On univariate analysis, significant differences were observed between the good and poor prognosis groups (Table IV; Fig. 2).

In the Cox's regression multivariate analysis, high pT and advanced TNM stage, but not tumor size, pN category or the prognosis group, could be proven as independent predictors of short OS and RFS (Table V).

TABLE I. Correlation of p16, Cyclin D1, CDK4, and pRb Expression

	n	p16+	Cyclin D1+	CDK4+	pRb+
p16					
+	81	Blank	28 (35)	35 (43)	57 (70)
−	77	Blank	30 (40)	24 (31)	38 (49)
			$P=0.622$	$P=0.140$	$P=0.009$
Cyclin D1					
+	58	28 (48)	Blank	26 (45)	38 (66)
−	100	53 (53)	Blank	33 (33)	57 (57)
		$P=0.622$		$P=0.173$	$P=0.316$
CDK4					
+	59	35 (59)	26 (44)	Blank	39 (66)
−	99	46 (47)	32 (32)	Blank	56 (57)
		$P=0.140$	$P=0.173$		$P=0.246$
pRb					
+	95	57 (60)	38 (40)	39 (41)	Blank
−	63	24 (38)	20 (32)	20 (32)	Blank
		$P=0.009$	$P=0.316$	$P=0.246$	

Values in parenthesis are percentage.

DISCUSSION

We found that most gastric carcinoma exhibit abnormal expression of at least one of the four genes studied here; loss of p16/Rb and overexpression of cyclin D1/CDK4 each occurred in about 40–50% of the cases. Although alteration of each individually did not show influence, combination of p16, pRb, cyclin D1, and CDK4 expression yielded additional prognostic information.

p16 Expression in Gastric Mucosa Might be Complex

The present study showed p16 to be generally expressed at very low levels in normal gastric epithelium, with relatively strong expression at

TABLE II. Expression of p16, Cyclin D1, CDK4, and pRb in Correlation With Clinicopathological Variables

Variable	n	p16 −ve	*P*-value	Cyclin D1 +ve	*P*-value	CDK4 +ve	*P*-value	pRb −ve	*P*-value
Sex									
Female	50	29 (58)	0.126	20 (40)	0.597	23 (46)	0.157	21 (42)	0.730
Male	108	48 (44)		38 (35)		36 (33)		42 (39)	
Age									
≤65	61	30 (49)	>0.999	25 (41)	0.401	21 (17)	0.614	25 (41)	0.868
>65	97	47 (49)		33 (34)		38 (21)		38 (39)	
Size (cm)									
≤5.0	83	42 (51)	0.636	36 (43)	0.072	31 (37)	>0.999	32 (39)	0.747
>5.0	75	35 (47)		22 (29)		28 (37)		31 (41)	
Location									
Upper	21	13 (62)	0.188	10 (48)	0.515	9 (43)	0.783	10 (48)	0.239
Middle	69	36 (52)		25 (36)		24 (35)		31 (45)	
Lower	68	28 (41)		23 (34)		26 (38)		22 (32)	
Laurén									
Intestinal	86	36 (42)	0.088	32 (37)	>0.999	32 (37)	>0.999	27 (31)	0.022
Diffuse	72	41 (57)		26 (36)		27 (38)		36 (50)	
pT									
T1	72	34 (47)	0.918	31 (43)	0.124	36 (50)	0.008	24 (33)	0.307
T2	55	27 (49)		18 (33)		13 (24)		25 (46)	
T3	31	16 (52)		9 (29)		10 (32)		14 (45)	
pN									
N0	97	46 (47)	0.745	42 (43)	0.042	42 (43)	0.063	36 (37)	0.407
N1-3	61	31 (51)		16 (26)		17 (28)		27 (44)	
TNM stage									
I/II	127	60 (47)	0.549	51 (40)	0.096	51 (40)	0.153	50 (39)	0.839
III/IV	31	17 (55)		7 (23)		8 (26)		13 (42)	

Values in parenthesis are percentage. Laurén, Laurén's classification.

the bottoms of the regenerative glands, in line with previous reports [7,8]. These findings suggest that in regenerative mucosa p16 may suppress abnormally enhanced cell cycle turnover as a negative feedback or homeostatic mechanism. However, the antigen expression in gastric carcinomas might be more complex: 77 of our 158 (49%) gastric carcinoma cases showed loss of expression of p16 whereas relatively high levels (>30%) of expression were seen in 31 (20%) tumors. Indeed, p16 expression has been reported to be increased in gastric carcinomas [9–11], as also found by Western blotting [8]. Similarly, p16 mRNA levels may be higher in some colorectal carcinomas than in matched normal mucosa [12,13]. In vitro, activation of *ras* and the mitogen-activated protein kinase pathway has been shown to increase p16 expression [14,15]. It seems therefore likely that multiple events influence enhanced p16 expression in gastric carcinomas.

The reported prevalence of p16 loss in gastric carcinoma is 11–53% [4,7–11,16–19]. Homozygous deletions and mutations of the p16 gene are rare, in the range from 0% to 13% [9,20] whereas hypermethylation in the gene promoter region accounts for inactivation in 18–87% of cases [16,21,22,19]. Gastric carcinoma tissues with p16 promoter methylation express significantly lower levels of p16 protein [8,20,22,23]. As assessed by Northern blot analysis, gastric carcinoma cell lines reexpress p16 mRNA when treated with the demethylating agent 5-aza-2′-deoxycytidine [20]. These data support the idea that hypermethylation in the p16 gene promoter region is responsible for the loss of p16 expression in gastric carcinomas. In previous studies, p16 expression was associated with lymph node metastasis [10,17], histologic type [8,10], and location [7,18]. In addition, existing data suggest that loss of p16 plays a role in the pathogenesis of Epstein–Barr virus-associated gastric carcinomas [7,23]. However, no correlation was found with any of the available clinicopathological parameters in the present or other studies [4,11,23].

Loss of pRb Expression Associated With the Histological Type of Laurén

Decrease or loss of pRb expression has been found in gastric carcinoma as compared to the diffuse positivity in non-neoplastic mucosa [3,4,10] with a prevalence in the range from 4% to 56% [3,4,10,24–26]. Our study demonstrated pRb in over 50% of cells in normal, regenerative and metaplastic epithelium, whereas the figure was less than 5% in 40% of the tumors. Loss of pRb expression was more prevalent in the diffuse type gastric carcinomas in the present study, in line with the earlier report of high pRb expression in intestinal type tumors [11]. The depth of tumor invasion, lymph node metastasis or prognosis has been documented to be associated with loss of pRb [4,24–26] although no significant influence of pRb status on clinicopathological parameters was evident in the present and other studies [3,8].

Positive Link Between p16 and pRb Expression

It has been proposed that physiological inactivation of pRb during the G1-phase leads to increased p16 expression [1]. This negative feedback model predicts that pRb-negative tumors would have high levels of p16, while pRb-positive tumors might require decreased amounts of functional p16 vice versa. Indeed, an inverse relationship exists between pRb and p16 expression in gastric carcinomas [10,11]. However, we have observed a positive link between the two proteins in agreement with another study [3]. In addition, no reciprocal expression was apparent in two studies [4,8]. These conflicting results may reflect differences in methodology such as antibodies used or cutoff values for immunoreactivity. Further analysis at the mRNA level may be necessary for clarification.

TABLE III. Univariate Analysis of Clinicopathological Features and Immunohistochemical Results With Reference to Overall and Recurrence-Free Survival

Variable	n	OS	HR (95% CI)	*P*-value	RFS	HR (95% CI)	*P*-value
Sex							
Female	50	44 (86)	1		43 (85)	1	
Male	108	85 (68)	1.736 (0.707–4.263)	NS	85 (75)	1.527 (0.655–3.559)	NS
Age							
≤65	61	51 (70)	1		51 (79)	1	
>65	97	78 (75)	1.321 (0.613–2.846)	NS	77 (78)	1.326 (0.621–2.834)	NS
Size (cm)							
≤5.0	83	74 (87)	1		75 (90)	1	
>5.0	75	54 (58)	3.653 (1.614–8.268)	0.002	53 (65)	3.548 (1.578–7.977)	0.002
Location							
Upper	21	16 (69)	1		16 (73)	1	
Middle	69	57 (76)	0.606 (0.213–1.724)	NS	57 (79)	0.601 (0.212–1.707)	NS
Lower	68	56 (71)	0.723 (0.255–2.056)	NS	55 (78)	0.704 (0.251–1.977)	NS
Laurén							
Intestinal	86	74 (80)	1		74 (85)	1	
Diffuse	72	55 (65)	1.830 (0.874–3.833)	NS	54 (70)	1.951 (0.940–4.052)	0.073
pT							
T1	72	70 (95)	1		70 (97)	1	
T2	55	45 (73)	6.860 (1.500–31.379)	0.013	44 (78)	8.246 (1.826–37.240)	0.006
T3	31	14 (26)	30.652 (7.045–133.361)	<0.001	14 (33)	28.101 (6.457–121.969)	<0.001
pN							
N0	97	90 (88)	1		90 (90)	1	
N1-3	61	39 (51)	6.068 (2.589–14.224)	<0.001	38 (58)	6.315 (2.707–14.731)	<0.001
TNM stage							
I/II	127	117 (86)	1		117 (90)	1	
III/IV	31	12 (16)	13.806 (6.282–30.340)	<0.001	11 (31)	12.678 (5.877–27.350)	<0.001
p16							
+	81	68 (74)	1		68 (80)	1	
−	77	61 (73)	1.322 (0.635–2.751)	NS	60 (76)	1.467 (0.712–3.021)	NS
Cyclin D1							
+	58	48 (78)	1		48 (82)	1	
−	100	81 (70)	1.360 (0.631–2.932)	NS	80 (75)	1.263 (0.591–2.701)	NS
CDK4							
+	59	53 (86)	1		52 (87)	1	
−	99	76 (68)	1.935 (0.786–4.762)	NS	76 (74)	1.874 (0.803–4.370)	NS
pRb							
+	95	80 (77)	1		79 (81)	1	
−	63	49 (70)	1.085 (0.522–2.256)	NS	49 (75)	1.233 (0.601–2.533)	NS

Values in parenthesis are percentage. OS, overall survival; RFS, recurrence-free survival; HR, hazard ratio; CI, confidence interval; Laurén, Laurén's classification; NS, not significant.

TABLE IV. Univariate Analysis of the Relationship Between Survival and the Prognosis Group

Prognosis group	p16	Cyclin D1	CDK 4	pRb	n	n (total)	OS	OS (total)	HR (95% CI)	*P*-value	RFS (total)	HR (95% CI)	*P*-value	
Good						89		86%	1			87%	1	
	+	+	+	−	2		100%				100%			
	−	−	+	−	3		100%				100%			
	−	−	+	+	9		100%				89%			
	+	−	−	+	22		88%				86%			
	+	−	+	+	12		88%				88%			
	+	−	+	−	9		88%				88%			
	−	+	+	+	6		83%				83%			
	−	+	−	−	9		83%				89%			
	+	+	−	+	11		80%				81%			
Intermediate						45		70%	2.359 (0.977–5.695)	0.056		73%	2.151 (0.166–8.388)	0.073
	+	+	+	+	12		73%				80%			
	−	+	−	+	9		71%				76%			
	+	+	−	−	3		67%				67%			
	−	−	−	−	21		67%				68%			
Poor						24		33%	3.975 (1.576–10.021)	0.003		56%	3.011 (1.211–7.488)	0.018
	−	−	−	+	14		53%				67%			
	+	−	−	−	10		27%				47%			

OS, overall survival; RFS, recurrence-free survival; HR, hazard ratio; CI, confidence interval.

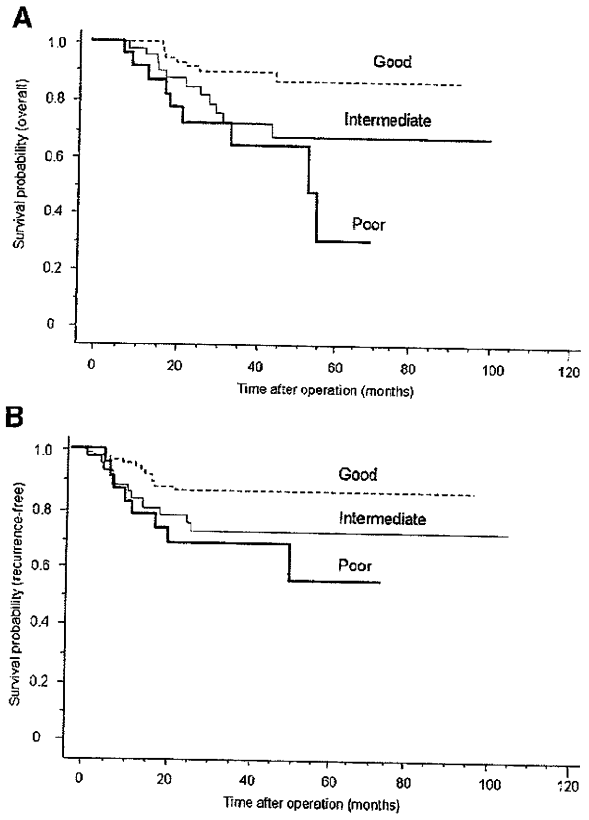

Fig. 2. Kaplan–Meier curves showing overall (A) and recurrence-free (B) survival with reference to the prognosis group.

Inverse Relationship Between Cyclin D1 Expression and Lymph Node Metastasis

We observed only weak or undetectable staining for cyclin D1 in non-neoplastic mucosa in line with previous reports [27–30]. None of a series of samples from normal gastric mucosa displayed cyclin D1 gene gain in an earlier report [29]. Conversely, strong immunoreactivity was apparent in 37% of gastric carcinomas in the present study. Cyclin D1 was previously studied in several series of gastric carcinomas [4,27–34], a 20–56% with frequency of overexpression being reported, in accordance with the present result. Cyclin D1 mRNA overexpression has been observed in 35–41% of gastric carcinomas [28,33], in line with protein overexpression. High levels of amplification or high-balanced polysomy of the cyclin D1 gene were also identified in 25% of cases [29]. We found cyclin D1 overexpression to be more prevalent in node-negative than in node-positive cases in agreement with an earlier report [33]. In addition, cyclin D1 overexpression has been found to be associated with higher age [31], poorly differentiated/signet ring cell type [4], papillary and well to moderately differentiated/intestinal type [27,30], early stage cancer [3] and a poor prognosis [28]. Thus, clinicopathological association with its protein expression still remains controversial.

Inverse Relationship Between CDK4 Expression and Lymph Node Metastasis

CDK4 expression was previously studied in limited series of gastric carcinomas [3,31,33]; 48–100% cases were estimated to be protein overexpressers, and 45% overexpressed CDK4 mRNA. In our cases, no expression of CDK4 was apparent in non-neoplastic mucosa although distinct nuclear/cytoplasmic staining was identified in 37% of the gastric carcinomas. While we found an inverse relationship between CDK4 expression and depth of tumor invasion, the antigen was reported to be expressed equally in early and advanced gastric carcinomas [3]. CDK4 overexpression may be apparently linked to vessel invasion, poor prognosis and cyclin D1 expression [31,33] although this could not be confirmed in the present study.

Disruption of Rb Pathway in Gastric Carcinomas

Associations between p16, Rb, cyclin D1 and CDK4 have not been assessed previously in large series of gastric carcinoma cases. In 86% of these in the present study, abnormal expression of at least 1 protein was found, implying disruption of the pRb cell cycle control pathway. This percentage is similar to the prevalence of 92% reported in gastric carcinomas in a previous study of 3 proteins (p16/Rb/cyclin D1) [4]. The fact that 14% of our tumors retained normal expression (p16+/Rb+/cyclin D1−/CDK4−), suggested that other cell cycle regulator proteins might also play roles in pathogenesis or progression of gastric carcinomas.

Prognostic Impact of Immunohistochemical Marker Profiles

Our analysis of combination of p16, pRb, cyclin D1, and CDK4 expression yielded additional prognostic information; patients with p16+/pRb−/cyclin D1−/CDK4− or p16−/pRb+/cyclin D1−/CDK4− tumors demonstrated particularly poor survival. This was the most relevant combination of alteration contributing to a poor prognosis, whereas alteration of each individually did not show influence. Conversely, patients with p16+/pRb−/cyclin D1+/CDK4+,

TABLE V. Multivariate Cox Proportional Hazards Analysis of the Relationship Between Survival and Variables Selected by Univariate Analysis

	OS		RFS	
Variable	HR (95% CI)	*P*-value	HR (95% CI)	*P*-value
pT				
T1	1		1	
T2	5.160 (1.100–24.198)	0.038	12.575 (1.594–99.183)	0.016
T3	8.499 (1.578–45.776)	0.013	12.068 (1.340–108.691)	0.026
TNM stage				
I/II	1		1	
III/IV	5.822 (2.121–15.981)	0.001	7.431 (2.596–21.276)	<0.001

OS, overall survival; RFS, recurrence-free survival; HR, hazard ratio; CI, confidence interval.

p16−/pRb+/cyclin D1−/CDK4+ or p16−/pRb−/cyclin D1−/CDK4+ tumors were all alive. These results raise the possibility that specific marker profiles could contribute significantly to future clinical management in gastric carcinoma patients.

ACKNOWLEDGMENTS

We thank Y. Oya, J. Kubo and N. Anpo, Pathology Division, National Hospital Organization Sagamihara Hospital, for their expert technical assistance. This work was supported by a Grant-in-Aid from the Parents' Association Grant (Keyaki-kai) of Kitasato University, School of Medicine.

REFERENCES

1. Serrano M, Hannon GJ, Beach D: A new regulatory motif in cell-cycle control causing specific inhibition of cyclin D/CDK4. Nature 1993;366:704–707.
2. Weinberg RA: The retinoblastoma protein and cell cycle control. Cell 1995;81:323–330.
3. Myung N, Kim MR, Chung IP, et al.: Loss of p16 and p27 is associated with progression of human gastric cancer. Cancer Lett 2000;153:129–136.
4. Feakins RM, Nickols CD, Bidd H, et al.: Abnormal expression of pRb, p16, and cyclin D1 in gastric adenocarcinoma and its lymph node metastases: Relationship with pathological features and survival. Hum Pathol 2003;34:1276–1282.
5. Laurén P: The two histological main types of gastric carcinoma: Diffuse and so-called intestinal-type carcinoma. Acta Path Microbiol Scandinav 1965;64:31–49.
6. Sobin LH, Wittekind CH, editors. TNM classification of malignant tumours. 6th edition. New York: Wiley-Liss; 2002.
7. Schneider BG, Gulley ML, Eagan P, et al.: Loss of p16/CDKN2A tumor suppressor protein in gastric adenocarcinoma is associated with Epstein-Barr virus and anatomic location in the body of the stomach. Hum Pathol 2000;31:45–50.
8. Tsujie M, Yamamoto H, Tomita N, et al.: Expression of tumor suppressor gene $p16^{INK4}$ products in primary gastric cancer. Oncology 2000;58:126–136.
9. Zhao G-H, Li T-C, Shi L-H, et al.: Relationship between inactivation of p16 gene and gastric carcinoma. World J Gastroenterol 2003;9:905–909.
10. He X-S, Rong Y-H, Su Q, et al.: Expression of *p16* gene and Rb protein in gastric carcinoma and their clinicopathological significance. World J Gastroenterol 2005;11:2218–2223.
11. Mattioli E, Vogiatzi P, Sun A, et al.: Immunohistochemical analysis of pRb2/p130, VEGF, EZH2, p53, $p16^{INK4A}$, $p27^{KIP1}$, $p21^{WAF1}$, Ki-67 expression patterns in gastric cancer. J Cell Physiol 2007;210:183–191.
12. Ohhara M, Esumi M, Kurosu Y: Activation but not inactivation of the *MTS1* gene is associated with primary colorectal carcinomas. Biochem Biophys Res Commun 1996;226:791–795.
13. Dai CY, Furth EE, Mick R, et al.: p16 ^{INK4a} expression begins early in human colon neoplasia and correlates inversely with markers of cell proliferation. Gastroenterology 2000;119:929–942.
14. Serrano M, Lin AW, McCurrach ME, et al.: Oncogenic *ras* provokes premature cell senescence associated with accumulation of p53 and p16 ^{INK4a}. Cell 1997;88:593–602.
15. Lin AW, Barradas M, Stone JC, et al.: Premature senescence involving p53 and p16 is activated in response to constitutive MEK/MAPK mitogenic signaling. Genev Dev 1998;12:3008–3019.
16. Shim Y-H, Kang GH, Ro JY: Correlation of *p16* hypermethylation with p16 protein loss in sporadic gastric carcinomas. Lab Invest 2000;80:689–695.
17. Honda T, Tamura G, Endoh Y, et al.: Expression of tumor suppressor and tumor-related proteins in differentiated carcinoma, undifferentiated carcinoma with tubular component and pure undifferentiated carcinoma of the stomach. Jpn J Clin Oncol 2005;35:580–586.
18. Kim MA, Lee HS, Yang H-K, et al.: Clinicopathologic and protein expression differences between cardia carcinoma and noncardia carcinoma of the stomach. Cancer 2005;103:1439–1446.
19. Song SH, Jong H-S, Choi HH, et al.: Methylation of specific CpG sites in the promoter region could significantly down-regulate $p16^{INK4a}$ expression in gastric adenocarcinoma. Int J Cancer 2000;87:236–240.
20. Lee YY, Kang SH, Seo JY, et al.: Alterations of $p16^{INK4A}$ and $p15^{INK4B}$ genes in gastric carcinomas. Cancer 1997;80:1889–1896.
21. Oue N, Oshimo Y, Nakayama H, et al.: DNA methylation of multiple genes in gastric carcinoma: association with histological type and CpG island methylator phenotype. Cancer Sci 2003;94:901–905.
22. Hou P, Ji M-J, Shen J-Y, et al.: Detection of *p16* hypermethylation in gastric carcinomas using a seminested methylation-specific PCR. Biochem Genet 2005;43:1–9.
23. Osawa T, Chong J-M, Sudo M, et al.: Reduced expression and promoter methylation of *p16* gene in Epstein-Barr virus-associated gastric carcinoma. Jpn J Cancer Res 2002;93:1195–1200.
24. Song HS, Kim IH, Sohn SS, et al.: Prognostic significance of immunohistochemical expression of p53 and retinoblastoma gene protein (pRb) in curatively resected gastric cancer. Korean J Intern Med 2005;20:1–7.
25. Chou N-H, Chen H-C, Chou N-S, et al.: Expression of altered retinoblastoma protein inversely correlates with tumor invasion in gastric carcinoma. World J Gastroenterol 2006;12:7188–7191.
26. Songun I, van de Velde CJH, Hermans J, et al.: Expression of oncoproteins and the amount of eosinophilic and lymphocytic infiltrates can be used as prognostic factors in gastric cancer. Dutch Gastric Cancer Group (DGCG). Br J Cancer 1996;74:1783–1788.
27. Müller W, Noguchi T, Wirtz H-C, et al.: Expression of cell-cycle regulatory proteins cyclin D1, cyclin E, and their inhibitor p21 waf1/cip1 in gastric cancer. J Pathol 1999;189:186–193.
28. Gao P, Zhou G-Y, Liu Y, et al.: Alteration of cyclin D1 in gastric carcinoma and its clinicopathologic significance. World J Gastroenterol 2004;10:2936–2939.
29. Bizari L, Borim AA, Leite KRM, et al.: Alterations of the CCND1 and HER-2/neu (ERBB2) proteins in esophageal and gastric cancers. Cancer Genet Cytogenet 2006;165:41–50.
30. Arber N, Gammon MD, Hibshoosh H, et al.: Overexpression of cyclin D1 occurs in both squamous carcinomas and adenocarcinomas of the esophagus and in adenocarcinomas of the stomach. Hum Pathol 1999;30:1087–1092.
31. Takano Y, Kato Y, Masuda M, et al.: Cyclin D2, but not cyclin D1, overexpression closely correlates with gastric cancer progression and prognosis. J Pathol 1999;189:194–200.
32. Han S, Kim H-Y, Park K, et al.: Expression of p27Kip1 and cyclin D1 proteins is inversely correlated and is associated with poor clinical outcome in human gastric cancer. J Surg Oncol 1999;71:147–154.
33. Takano Y, Kato Y, van Diest PJ, et al.: Cyclin D2 overexpression and lack of p27 correlate positively and cyclin E inversely with a poor prognosis in gastric cancer cases. Am J Pathol 2000;156:585–594.
34. Tenderenda M: A study on the prognostic value of cyclins D1 and E expression levels in resectable gastric cancer and on some correlations between cyclins expression, histoclinical parameters and selected protein products of cell-cycle regulatory genes. J Exp Clin Cancer Res 2005;24:405–414.

Synopsis for Table of Contents

Our immunohistochemical analysis demonstrated that the Rb pathway is disrupted in the vast majority of gastric carcinomas. This study also identified specific immunohistochemical marker profiles for prognosis.

ARTHRITIS & RHEUMATISM
Vol. 58, No. 12, December 2008, pp 3843–3853
DOI 10.1002/art.24036

Zonal Gene Expression of Chondrocytes in Osteoarthritic Cartilage

Naoshi Fukui,[1] Yoshinari Miyamoto,[2] Masahiro Nakajima,[2] Yasuko Ikeda,[1] Atsuhiko Hikita,[1] Hiroshi Furukawa,[1] Hiroyuki Mitomi,[1] Nobuho Tanaka,[1] Yozo Katsuragawa,[3] Seizo Yamamoto,[4] Motoji Sawabe,[4] Takuo Juji,[1] Toshihito Mori,[1] Ryuji Suzuki,[1] and Shiro Ikegawa[2]

Objective. **To determine the chondrocyte metabolism in respective zones of osteoarthritic (OA) cartilage.**

Methods. **OA cartilage was obtained from macroscopically intact areas of 4 knee joints with end-stage OA. The cartilage was divided into 3 zones, and gene expression profiles were determined in the respective zones by a custom-designed microarray that focused on chondrocyte-related genes. For the genes whose expression was significantly different among the zones, the expression was compared between OA and control cartilage in the respective zones by an analysis using laser capture microdissection and real-time polymerase chain reaction (PCR). For some genes, the correlation of expression was investigated in specific cartilage zones.**

Results. **A total of 198 genes (~40% of those investigated) were found to be expressed at significantly different levels among the zones. Expression of 26 of those genes was evaluated by laser capture microdissection and real-time PCR, which confirmed the validity of microarray analysis. The expression of cartilage matrix genes was mostly enhanced in OA cartilage, at similar levels across the zones but at different magnitudes among the genes. The expression of bone-related genes was induced either in the superficial zone or in the deep zone, and positive correlations were found among their expression in the respective zones. The expression of 5 proteinase genes was most enhanced in the superficial zone, where their expression was correlated, suggesting the presence of a common regulatory mechanism(s) for their expression.**

Conclusion. **In OA cartilage, the metabolic activity of chondrocytes differed considerably among zones. Characteristic changes were observed in the superficial and deep zones.**

Osteoarthritis (OA) is the most prevalent joint disease in developed countries that primarily affects articular cartilage. In OA, cartilage matrix is lost gradually, which eventually devastates functional joints. Chondrocytes are the sole type of cells that reside in articular cartilage. Currently, they are considered to play a pivotal role in progression of OA. Chondrocytes express catabolic cytokines and proteinases that promote loss of cartilage matrix (1). Chondrocytes undergo phenotypic changes and come to express matrix genes that are little expressed in normal articular cartilage (2–4). This induction of noncartilaginous matrices could facilitate the loss of cartilage matrix by altering the composition and properties of the matrix (5). Thus, in order to understand the pathology of OA, it is crucially important to know how the chondrocyte metabolism is altered within OA cartilage.

Articular cartilage is a highly organized tissue. Based on histologic features, the articular cartilage

Dr. Fukui's work was supported by Grants-in-Aid from the Japan Society for the Promotion of Science (grants 15390467 and 18390424), the Ministry of Health, Labor and Welfare of Japan (grant 200500734A), and the Uehara Memorial Foundation.

[1]Naoshi Fukui, MD, PhD, Yasuko Ikeda, DVM, Atsuhiko Hikita, MD, PhD, Hiroshi Furukawa, MD, PhD, Hiroyuki Mitomi, MD, PhD, Nobuho Tanaka, MS, Takuo Juji, MD, Toshihito Mori, MD, Ryuji Suzuki, DVM, PhD: National Hospital Organization Sagamihara Hospital, Kanagawa, Japan; [2]Yoshinari Miyamoto, MD, Masahiro Nakajima, BS, Shiro Ikegawa, MD, PhD: SNP Research Center, RIKEN, Tokyo, Japan; [3]Yozo Katsuragawa, MD: International Medical Center of Japan, Tokyo, Japan; [4]Seizo Yamamoto, MD, PhD, Motoji Sawabe, MD, PhD: Tokyo Metropolitan Geriatric Hospital, Tokyo, Japan.

Address correspondence and reprint requests to Naoshi Fukui, MD, PhD, Clinical Research Center, National Hospital Organization Sagamihara Hospital, Sakuradai 18-1, Sagamihara, Kanagawa 228-8522, Japan (e-mail: n-fukui@sagamihara-hosp.gr.jp); or to Shiro Ikegawa, MD, PhD, Laboratory for Bone and Joint Diseases, SNP Research Center, RIKEN, Shirokanedai 4-6-1, Minato-ku, Tokyo 108-8639, Japan (e-mail: sikegawa@ims.u-tokyo.ac.jp).

Submitted for publication March 4, 2008; accepted in revised form August 11, 2008.

above the tidemark is divided into 3 distinct layers, the superficial, middle, and deep zones (6,7), in which the morphology and density of chondrocytes differ (8). The composition of cartilage matrix also differs among the zones. While the superficial zone is rich in collagens, the middle and deep zones contain more proteoglycan than the superficial zone (9). Corresponding to these differences, the chondrocyte metabolism differs considerably among the zones (2). The regional difference in chondrocyte metabolism may be even more important in the analysis of OA pathology. In the early stage of OA, chondrocytes in the superficial zone could be catabolically more active, which initiates cartilage degeneration at the surface areas (10–12).

In the present study, we attempted to determine the metabolic activity of chondrocytes in the respective zones of OA cartilage. Cartilage samples were obtained from macroscopically intact areas, and gene expression profiles of chondrocytes were determined by complementary DNA (cDNA) microarray that focused on chondrocyte-related genes. Comparison of gene expression profiles among the zones clarified the difference in cellular metabolism among the zones. Based on this result, gene expression was investigated in the respective zones of OA and control cartilage by an analysis using laser capture microdissection and real-time polymerase chain reaction (PCR) (2,13). The results of these analyses revealed previously unrecognized features of the chondrocyte metabolism in OA cartilage.

MATERIALS AND METHODS

Cartilage. The study was performed with the approval of the Human Ethics Review Committees of the institutes that participated in the study, and informed consent was obtained in writing from each subject or family of the donor before material collection. All OA cartilage was obtained from knees with end-stage OA at prosthetic surgery. The diagnosis of OA was based on the criteria for knee OA of the American College of Rheumatology (14). The cartilage was obtained from knees with medial involvement, and cartilage from laterally or bilaterally involved knees was not used for this study. For microarray analysis, OA cartilage was obtained from 4 OA knee joints in 4 patients (mean age 73.2 years, range 62–82 years). The cartilage was taken from the weight-bearing area of a lateral femoral condyle, where cartilage presented few signs of macroscopic degeneration. Cartilage was harvested in a square of 15–20 mm on a side, in full thickness above the tidemark. After harvest, the cartilage was separated into superficial, middle, and deep zones with a scalpel under a dissection microscope. The separated cartilages were each embedded in OCT compound (Sakura Finetek, Tokyo, Japan), snap-frozen in liquid nitrogen, and stored at −80°C until analysis. This processing of cartilage was completed within 4 hours after the acquisition.

Table 1. Abundance of gene expression in the superficial zone compared with that in the middle zone*

Gene symbol	Accession no.	Gene name	Signal intensity		Signal ratio†
			Superficial zone	Middle zone	
Greater expression in superficial zone					
CRABP2	NM_001878.2	Cellular retinoic acid binding protein 2	4.230×10^1	7.578×10^0	5.582
TNFAIP6	NM_007115.2	Tumor necrosis factor α–induced protein 6	8.398×10^2	2.370×10^2	3.543
MATN4	NM_003833.2	Matrilin 4, transcript variant 1	8.317×10^2	2.401×10^2	3.464
TNA	NM_003278.1	Tetranectin	3.155×10^3	1.032×10^3	3.057
WNT5B	NM_030775.2	Wingless-type MMTV integration site family, member 5B, transcript variant 2	3.733×10^1	1.340×10^1	2.786
MMP13	NM_002427.2	Matrix metalloproteinase 13	5.177×10^2	1.901×10^2	2.724
POSTN	NM_006475.1	Periostin, osteoblast-specific factor	7.608×10^2	3.156×10^2	2.411
DAF	NM_000574.2	Decay-accelerating factor for complement (CD55)	2.276×10^3	1.098×10^3	2.072
TIMP3	NM_000362.3	Tissue inhibitor of metalloproteinase 3	1.745×10^3	8.546×10^2	2.042
Greater expression in middle zone					
COL10A1	NM_000493.2	Collagen, type X, α1	4.840×10^0	5.309×10^1	0.091
LECT1	NM_007015.1	Leukocyte cell–derived chemotaxin 1	9.141×10^1	4.027×10^2	0.227
FGF13	NM_004114.2	Fibroblast growth factor 13, transcript variant 1A	4.701×10^1	1.458×10^2	0.322
CHAD	NM_001267.1	Chondroadherin	2.837×10^3	8.609×10^3	0.330
MATN3	NM_002381.3	Matrilin 3	6.803×10^1	1.725×10^2	0.394
ITM2A	NM_004867.2	Integral membrane protein 2A	6.745×10^2	1.566×10^3	0.431
MMP9	NM_004994.1	Matrix metalloproteinase 9	3.995×10^1	8.900×10^1	0.449

* Genes whose signals in the superficial zone were ≥2 times those in the middle zone are shown in the order of signal intensity ratio. Genes whose signals in the superficial zone were ≤0.5 times those in the middle zone are shown in the order of signal intensity ratio.
† Signal intensity of the superficial zone relative to that of the middle zone.

Table 2. Abundance of gene expression in the middle zone compared with that in the deep zone*

Gene symbol	Accession no.	Gene name	Signal intensity		Signal ratio†
			Middle zone	Deep zone	
Greater expression in middle zone					
MMP13	NM_002427.2	Matrix metalloproteinase 13	1.889×10^2	2.852×10^1	6.625
C3	NM_000064.1	Complement component 3	1.209×10^2	1.950×10^1	6.199
FGF7	NM_002009.2	Fibroblast growth factor 7	2.553×10^1	7.617×10^0	3.352
COL12A1	NM_004370.4	Collagen, type XII, α1, transcript variant long	9.605×10^2	3.355×10^2	2.863
CHI3L1	NM_001276.1	Chitinase 3–like 1 (cartilage glycoprotein 39)	2.895×10^4	1.046×10^4	2.768
LAMA4	NM_002290.2	Laminin, α4	2.492×10^2	9.907×10^1	2.515
MMP2	NM_004530.1	Matrix metalloproteinase 2	7.357×10^2	3.005×10^2	2.448
CHI3L2	NM_004000.1	Chitinase 3–like 2	2.582×10^4	1.063×10^4	2.429
FAP	NM_004460.2	Fibroblast activation protein, α	7.107×10^2	2.932×10^2	2.424
TIMP1	NM_003254.1	Tissue inhibitor of metalloproteinase 1	2.664×10^4	1.114×10^4	2.392
GRM1	NM_000838.2	Glutamate receptor, metabotropic 1	4.149×10^1	1.736×10^1	2.390
MMP3	NM_002422.2	Matrix metalloproteinase 3	9.857×10^3	4.692×10^3	2.101
Greater expression in deep zone					
WNT5B	NM_030775.2	Wingless-type MMTV integration site family, member 5B, transcript variant 2	1.358×10^1	8.472×10^1	0.160
SPP1	NM_000582.2	Secreted phosphoprotein 1 (osteopontin, bone sialoprotein 1)	9.187×10^2	4.301×10^3	0.214
IBSP	NM_004967.2	Integrin-binding sialoprotein (bone sialoprotein, bone sialoprotein II)	1.791×10^2	6.609×10^2	0.271
TNFRSF11B	NM_002546.2	Tumor necrosis factor receptor superfamily, member 11b (osteoprotegerin)	3.485×10^2	1.081×10^3	0.322
MATN3	NM_002381.3	Matrilin 3	1.715×10^2	5.162×10^2	0.332
COL10A1	NM_000493.2	Collagen, type X, α1	5.325×10^1	1.422×10^2	0.374
SLC26A2	NM_000112.2	Solute carrier family 26, member 2	2.118×10^2	5.389×10^2	0.393
TNFAIP6	NM_007115.2	Tumor necrosis factor α–induced protein 6	2.352×10^2	5.207×10^2	0.452
PLOD2	NM_000935.1	Procollagen-lysine, 2-oxoglutarate 5-dioxygenase 2, transcript variant 2	1.005×10^3	2.100×10^3	0.479

* Genes whose signals in the middle zone were ≥2 times those in the deep zone are shown in the order of signal intensity ratio. Genes whose signals in the middle zone were ≤0.5 times those in the deep zone are shown in the order of signal intensity ratio.
† Signal intensity of the middle zone relative to that of the deep zone.

For laser capture microdissection analysis, OA cartilage was obtained from another 42 knees with end-stage OA in 41 patients (from both knees in the case of 1 patient) (mean age 67.2 years, range 62–77 years) in the manner described for the microarray analysis. Control cartilage was harvested from 13 non-OA knees of 10 donors (from both knees in the case of 3 donors) (mean age 78.6 years, range 68–93 years) at the weight-bearing areas in lateral femoral condyles. The donors had no known history of joint disease or trauma, and normality of the joint was confirmed macroscopically at material collection. Control cartilage was obtained even when some signs of degeneration were noticed as long as the degeneration was limited (superficial degeneration in <20% of total cartilage area) and the lateral femoral condyle was spared from degeneration. After harvest, cartilages were immediately embedded in OCT compound and stored at −80°C until use.

RNA extraction. RNA for microarray analysis was extracted from the cartilage tissues following a previously described method (15) with some modifications. Briefly, 20-μm–thick cryosections were made from cartilage in OCT compound, and these were placed immediately into TRIzol reagent (Invitrogen, Carlsbad, CA). During this process, 1 of

Table 3. Abundance of gene expression in the superficial zone compared with that in the deep zone*

Gene symbol	Accession no.	Gene name	Signal intensity		Signal ratio†
			Superficial zone	Deep zone	
Greater expression in superficial zone					
MMP13	NM_002427.2	Matrix metalloproteinase 13	5.098×10^2	2.852×10^1	17.878
MMP2	NM_004530.1	Matrix metalloproteinase 2	1.369×10^3	3.005×10^2	4.554
POSTN	NM_006475.1	Periostin, osteoblast-specific factor	7.476×10^2	2.455×10^2	3.046
COL12A1	NM_004370.4	Collagen, type XII, α1, transcript variant long	9.530×10^2	3.355×10^2	2.840
FAP	NM_004460.2	Fibroblast activation protein, α	8.224×10^2	2.932×10^2	2.805
GRM1	NM_000838.2	Glutamate receptor, metabotropic 1	4.839×10^1	1.736×10^1	2.788
MATN4	NM_003833.2	Matrilin 4, transcript variant 1	8.168×10^2	3.037×10^2	2.689
TMSB4X	NM_021109.2	Thymosin, β4, X-linked	3.945×10^3	1.509×10^3	2.614
CHI3L2	NM_004000.1	Chitinase 3–like 2	2.693×10^4	1.063×10^4	2.534
LAMA4	NM_002290.2	Laminin, α4	2.482×10^2	9.907×10^1	2.505
FGF7	NM_002009.2	Fibroblast growth factor 7	1.883×10^1	7.617×10^0	2.473
ECM1	NM_004425.2	Extracellular matrix protein 1, transcript variant 1	5.263×10^2	2.130×10^2	2.471
ADAMTS5	NM_007038.1	A disintegrin-like and metalloproteinase with thrombospondin type 1 motif, 5 (aggrecanase 2)	1.497×10^2	6.068×10^1	2.466
TNA	NM_003278.1	Tetranectin	3.076×10^3	1.261×10^3	2.439
CHI3L1	NM_001276.1	Chitinase 3–like 1 (cartilage glycoprotein 39)	2.539×10^4	1.046×10^4	2.427
ITGB5	NM_002213.3	Integrin, β5	3.480×10^3	1.447×10^3	2.406
THBS2	NM_003247.2	Thrombospondin 2	3.281×10^2	1.426×10^2	2.300
MMP11	NM_005940.2	Matrix metalloproteinase 11	5.007×10^2	2.262×10^2	2.214
TIMP1	NM_003254.1	Tissue inhibitor of metalloproteinase 1	2.454×10^4	1.114×10^4	2.203
COL1A2	NM_000089.3	Collagen, type I, α2	8.784×10^3	4.019×10^3	2.186
MMP3	NM_002422.2	Matrix metalloproteinase 3	1.012×10^4	4.692×10^3	2.157
TNC	NM_002160.1	Tenascin C	4.803×10^3	2.271×10^3	2.115
IGFBP5	NM_000599.2	Insulin-like growth factor binding protein 5	8.847×10^2	4.183×10^2	2.115
GADD45A	NM_001924.2	Growth arrest and DNA damage–inducible, α	6.081×10^2	2.925×10^2	2.079
PLTP	NM_006227.2	Phospholipid transfer protein, transcript variant 1	5.329×10^2	2.617×10^2	2.036

every 40–50 sections was picked up on glass slides and stained with HistoGene stain (Arcturus, Mountain View, CA), and the appropriateness of zonal separation was confirmed under a light microscope by histology (6,7) (examples of histologic staining are available at http://www.hosp.go.jp/~sagami/rinken/crc/index.html). For the sections made from the deep zone cartilage, contamination of the calcified zone was also ruled out. RNA was first recovered from the TRIzol reagent in the aqueous phase, then purified using the RNeasy Micro kit (Qiagen, Hilden, Germany). The quality and quantity of RNA were routinely evaluated on a spectrophotometer (SmartSpec Plus; Bio-Rad, Hercules, CA) and a Bioanalyzer 2100 using RNA 6000 Nano Chips (Agilent, Santa Clara, CA). The RNA samples were used for the microarray analysis with the conditions that the A260 nm:A280 nm ratio was ≥1.8 and the 28S:18S ratio was ≥1.4.

Microarray analysis. Microarray analysis was performed using a custom-designed oligonucleotide microarray carrying 527 chondrocyte-related genes and 11 housekeeping genes (see Supplementary Table 1, available in the online version of this article at http://www3.interscience.wiley.com/journal/76509746/home). The chondrocyte-related genes were selected based upon previously reported data (16,17). They included genes encoding various matrix components, catabolic proteinases, cytokines, chemokines, growth factors, and their related molecules. The microarray was prepared by GeneFrontier (Tokyo, Japan) following a previously described method (18). In detail, 12 perfect-match probes and 12 mismatch probes, each 24 bases long, were designed for each gene and were synthesized on a microarray platform by NimbleGen's photolithography technology (NimbleGen Systems, Madison, WI) (19). The perfect-match probes had the sequences that exactly matched the gene, while the mismatch probes contained 2 mismatch bases in the 24 bases (6th and 12th bases from the 5′ end).

The RNA was reverse-transcribed, labeled with Cy3 fluorescent dye, and used for hybridization. The hybridization was performed using a 12-well array system (Nimble Screen 12; NimbleGen Systems) following the manufacturer's protocol. This system allowed simultaneous hybridization of 12 different samples on a single glass slide. The hybridization signal for each probe set was determined by the difference in signal intensities between the perfect-match and mismatch probes, using NimbleScan software (NimbleGen Systems). Obtained

Table 3. (*Cont'd*)

Gene symbol	Accession no.	Gene name	Signal intensity		Signal ratio†
			Superficial zone	Deep zone	
Greater expression in deep zone					
COL10A1	NM_000493.2	Collagen, type X, α1	4.892×10^0	1.422×10^2	0.034
LECT1	NM_007015.1	Leukocyte cell–derived chemotaxin 1	9.089×10^1	7.028×10^2	0.129
MATN3	NM_002381.3	Matrilin 3	6.775×10^1	5.162×10^2	0.131
IBSP	NM_004967.2	Integrin-binding sialoprotein (bone sialoprotein, bone sialoprotein II)	1.010×10^2	6.609×10^2	0.153
SPP1	NM_000582.2	Secreted phosphoprotein 1 (osteopontin, bone sialoprotein I)	7.099×10^2	4.301×10^3	0.165
CHAD	NM_001267.1	Chondroadherin	2.767×10^3	1.167×10^4	0.237
SLC26A2	NM_000112.2	Solute carrier family 26, member 2	1.343×10^2	5.389×10^2	0.249
GPC5	NM_004466.3	Glypican 5	1.783×10^1	7.109×10^1	0.251
ITM2A	NM_004867.2	Integral membrane protein 2A	6.632×10^2	2.353×10^3	0.282
TNFRSF11B	NM_002546.2	Tumor necrosis factor receptor superfamily, member 11b (osteoprotegerin)	3.403×10^2	1.081×10^3	0.315
PLOD2	NM_000935.1	Procollagen-lysine, 2-oxoglutarate 5-dioxygenase 2, transcript variant 2	7.420×10^2	2.100×10^3	0.353
CILP	NM_003613.2	Cartilage intermediate-layer protein, nucleotide pyrophosphohydrolase	9.287×10^3	2.553×10^4	0.364
HAPLN1	NM_001884.2	Hyaluronan and proteoglycan link protein 1	1.604×10^3	4.162×10^3	0.385
GREM1	NM_013372.4	Gremlin 1 homolog, cysteine knot superfamily	9.244×10^2	2.340×10^3	0.395
FRZB	NM_001463.2	Frizzled-related protein	2.664×10^3	6.556×10^3	0.406
S100A1	NM_006271.1	S100 calcium binding protein A1	1.798×10^3	4.104×10^3	0.438
COL2A1	NM_033150.1	Collagen, type II, α1, transcript variant 2	1.811×10^4	4.077×10^4	0.444
COL11A1	NM_001854.2	Collagen, type XI, α1, transcript variant A	2.684×10^3	5.936×10^3	0.452
AGC1	NM_001135.1	Aggrecan 1, transcript variant 1	4.317×10^3	9.068×10^3	0.476
COL2A1	NM_001844.3	Collagen type II, α1, transcript variant 1	1.959×10^4	4.110×10^4	0.477
COL9A2	NM_001852.3	Collagen, type IX, α2	1.123×10^3	2.354×10^3	0.477
CPE	NM_001873.1	Carboxypeptidase E	3.402×10^2	6.999×10^2	0.486
SPARC	NM_003118.2	Secreted protein, acidic, cysteine-rich	1.985×10^3	4.071×10^3	0.488

* Genes whose signals in the superficial zone were ≥2 times those in the deep zone are shown in the order of signal intensity ratio. Genes whose signals in the deep zone were ≥2 times those in the superficial zone are shown in the order of singal intensity ratio.
† Signal intensity of the superficial zone relative to that of the deep zone.

data were normalized by Microarray Analysis Suite 5.0 software (Affymetrix, Santa Clara, CA).

Laser capture microdissection. Laser capture microdissection was performed by a previously described method (2). Briefly, frozen sections of 10–20-μm thickness were prepared in the plane perpendicular to the joint surface from the cartilage samples embedded in the OCT compound. For laser capture microdissection, the sections were first treated with 0.5*M* EDTA (pH 8.0) for 3 minutes, then dehydrated with graded concentrations of ethanol and clarified with xylene. All reagents were prepared RNase free, and the entire process was completed within 30 minutes to minimize RNA degradation.

Under a laser capture microdissection device (PixCell IIe; Arcturus), each frozen section was divided into cartilage zones based on histologic features (2,6,7) (an example of histologic staining is available at http://www.hosp.go.jp/~sagami/rinken/crc/index.html). At each tissue procurement, the appropriateness of zone isolation was confirmed on the laser capture microdissection device.

Analysis of gene expression by real-time quantitative PCR. The obtained tissue was immediately placed in the RNA extraction buffer contained in an RNeasy Micro kit, and RNA was extracted by the kit with a routine use of DNase I (Qiagen). Complementary DNA was synthesized using Sensiscript reverse transcriptase (Qiagen). Gene expression was evaluated quantitatively by real-time PCR on an ABI PRISM 7700 (Applied Biosystems, Foster City, CA) or a LightCycler (Roche Diagnostics, Basel, Switzerland). Gene-specific primers were prepared (see Supplementary Table 2, available in the online version of this article at http://www3.interscience.wiley.com/journal/76509746/home), and the PCR reaction was performed using QuantiTect SYBR Green PCR (Qiagen). During the reaction, the amount of PCR product was monitored by the fluorescence from SYBR Green dye that bound to the product.

The PCR protocol was common for all genes: 94°C for 15 minutes to activate *Taq* polymerase, then 40–50 cycles of 94°C for 15 seconds, melting temperature of the primers for 30

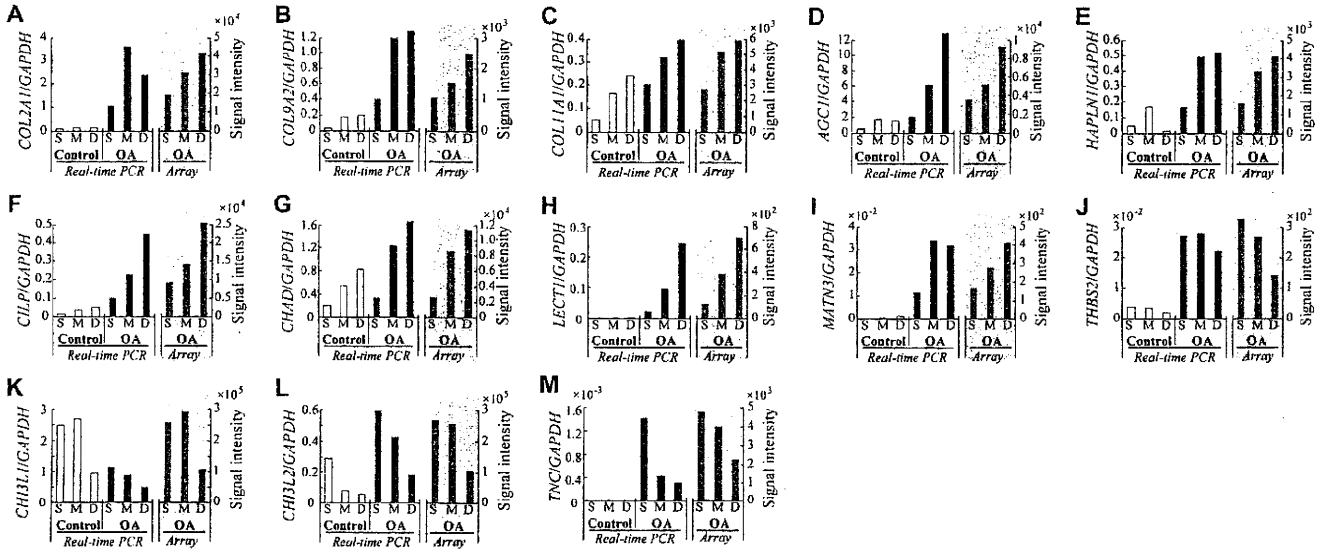

Figure 1. Comparison of cartilage matrix gene expression between microarray and real-time polymerase chain reaction (PCR) analyses. Expression of cartilage matrix genes was determined in superficial (S), middle (M), and deep (D) zones of osteoarthritic (OA) and control cartilage using laser capture microdissection and real-time PCR, and the result is shown together with that of the microarray analysis (Array). At least 8 samples were used for real-time PCR analysis. Results of real-time PCR analyses are shown as the ratio of the expression of the gene to that of *GAPDH*. Results of microarray analyses are shown as signal intensities. Expression of the following genes is shown: *COL2A1* (collagen, type II, α1) (**A**), *COL9A2* (collagen, type IX, α2) (**B**), *COL11A1* (collagen, type XI, α1) (**C**), *AGC1* (aggrecan 1) (**D**), *HAPLN1* (hyaluronan and proteoglycan link protein 1) (**E**), *CILP* (cartilage intermediate-layer protein, nucleotide pyrophosphohydrolase) (**F**), *CHAD* (chondroadherin) (**G**), *LECT1* (leukocyte cell–derived chemotaxin 1) (**H**), *MATN3* (matrilin 3) (**I**), *THBS2* (thrombospondin 2) (**J**), *CHI3L1* (chitinase 3–like 1 [cartilage glycoprotein 39]) (**K**), *CHI3L2* (chitinase 3–like 2) (**L**), *TNC* (tenascin C) (**M**).

seconds (see Supplementary Table 2, available in the online version of this article at http://www3.interscience.wiley.com/journal/76509746/home), and 72°C for 30 seconds. The amount of specific cDNA was quantified with a standard curve based on the known amounts of PCR product. The levels of cDNA among samples were normalized to the expression of GAPDH.

Statistical analysis. Statistically significant differences in gene expression between the zones were determined by 2-tailed *t*-test, and correlation of expression was evaluated by linear regression analysis. *P* values less than 0.05 were considered significant.

RESULTS

Microarray analysis findings. Significant levels of signals were obtained with all 538 probe sets (527 chondrocyte-related genes and 11 housekeeping genes) contained in the microarray. Among the 11 housekeeping genes, the expression of 4 genes (actin, beta; beta-2-microglobulin; phosphoglycerate kinase 1; transferrin receptor) was significantly different among cartilage zones. Thus, the normalization was performed on the expression of the remaining 7 housekeeping genes (glyceraldehyde-3-phosphate dehydrogenase; glucuronidase, beta; hypoxanthine phosphoribosyltransferase 1; peptidylprolyl isomerase A; ribosomal protein, large, P0; TATA box binding protein; 18S ribosomal RNA) (see Supplementary Table 1B, available in the online version of this article at http://www3.interscience.wiley.com/journal/76509746/home).

The expression of 198 of 527 chondrocyte-related genes was significantly different between any 2 cartilage zones. Between the superficial and middle zones, the expression of 93 genes was significantly different (see Supplementary Table 3, available in the online version of this article at http://www3.interscience.wiley.com/journal/76509746/home). Among them, 9 genes were expressed ≥2 times in the superficial zone, while another 7 genes were expressed ≥2 times in the middle zone (Table 1).

A total of 115 genes were expressed at significantly different levels between the middle and deep zones (see Supplementary Table 4, available in the online version of this article at http://www3.interscience.wiley.com/journal/76509746/home). The expression of 12 of them was increased ≥2-fold in the middle zone, while that of another 9 genes was increased ≥2-fold in the deep zone (Table 2). Among these genes, the expression of matrix metalloproteinase 13 (*MMP13*) was most increased in the middle zone, while the expres-

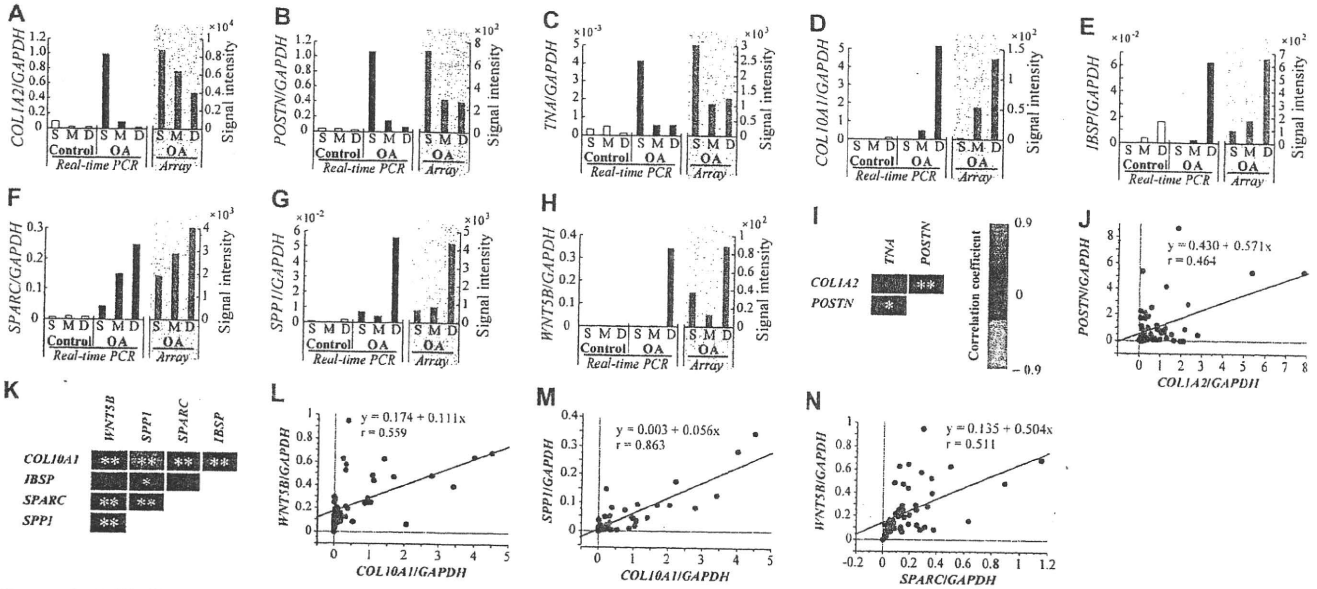

Figure 2. A–H, Comparison of bone-related gene expression between microarray and real-time PCR analyses. Expression of bone-related genes was determined in respective zones by laser capture microdissection and real-time PCR, and the result is shown together with that of the microarray analysis. Data are presented in the manner shown in Figure 1. At least 13 samples were used for real-time PCR analysis. **I–N,** Correlation of expression among the bone-related genes in OA cartilage. For genes primarily expressed in the superficial zone, correlation coefficients of expression are shown on a heat map (**I**), and the relationship of *POSTN* (periostin, osteoblast-specific factor) and *COL1A2* (collagen, type I, $\alpha 2$) expression is presented on a scattergram (**J**). For genes whose expression is most enhanced in the deep zone, correlation coefficients of expression are shown on a heat map (**K**), and relationships of expression between *COL10A1* (collagen, type X, $\alpha 1$) and *WNT5B* (wingless-type MMTV integration site family, member 5B, transcript variant 2), between *COL10A1* and *SPP1* (secreted phosphoprotein 1 [osteopontin, bone sialoprotein I]), and between *SPARC* (secreted protein, acidic, cysteine-rich) and *WNT5B* are shown on scattergrams (**L–N,** respectively). Results of 42 OA cartilage samples are shown. In **I** and **K,** red and green colors indicate positive and negative correlations, respectively. Expression of the following genes is also shown: *TNA* (tetranectin) (**C**), *IBSP* (integrin-binding sialoprotein [bone sialoprotein, bone sialoprotein II]) (**E**). * = $P < 0.05$; ** = $P < 0.01$. See Figure 1 for other definitions.

sion of wingless-type MMTV integration site family, member 5B, transcript variant 2 (*WNT5B*) was most enhanced in the deep zone.

The difference in gene expression was most obvious between the superficial and deep zones. The expression of 126 genes differed significantly between these zones (see Supplementary Table 5, available in the online version of this article at http://www3.interscience.wiley.com/journal/76509746/home). The expression of 25 of the 126 genes was increased ≥2 times in the superficial zone (Table 3). The expression of *MMP13* was most increased, followed by that of matrix metalloproteinase 2 (*MMP2*) and periostin, osteoblast-specific factor (*POSTN*). Meanwhile, the expression of another 23 genes was increased ≥2 times in the deep zone (Table 3). The expression of collagen, type X, $\alpha 1$ (*COL10A1*) was most increased (nearly 30 times), followed by that of leukocyte cell–derived chemotaxin 1 (*LECT1*), matrilin 3 (*MATN3*), integrin-binding sialoprotein (bone sialoprotein, bone sialoprotein II) (*IBSP*), and secreted phosphoprotein 1 (osteopontin, bone sialoprotein I) (*SPP1*).

Comparison of cartilage matrix gene expression between microarray analysis and real-time PCR. Real-time PCR analysis was performed on selected genes to validate the result of microarray analysis and to compare their expression in OA and control cartilage. Sixteen OA cartilage samples and 13 control cartilage samples were used for this analysis. Those cartilages were separated into 3 zones by laser capture microdissection for precise zone isolation based on their histologic features (2).

We chose a total of 26 genes for this analysis, considering the difference in expression levels among the zones (≥2-fold difference between any 2 zones), signal intensities, and relevance to OA pathology. These genes were categorized into 3 groups. The first group consisted of 13 genes encoding components of articular cartilage. The second group contained 8 genes that are expressed during hypertrophic change of the chondrocytes and those expressed by osteoblasts (bone-related

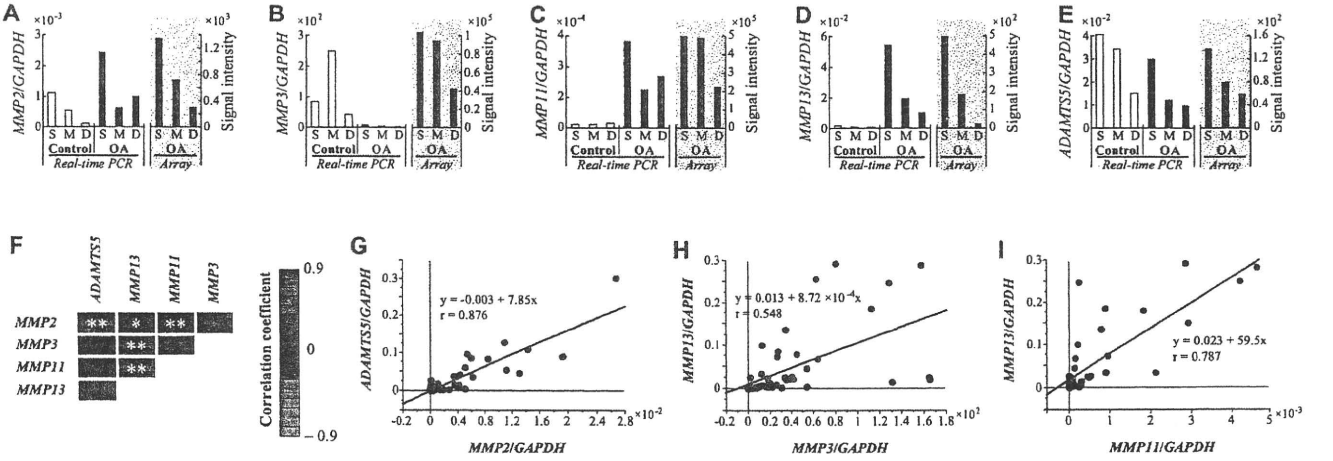

Figure 3. **A–E,** Comparison of metalloproteinase gene expression between microarray and real-time PCR analyses. Expression of bone-related genes was determined in respective zones by laser capture microdissection and real-time PCR, and the result is shown together with that of the microarray analysis. Data are presented in the manner shown in Figure 1. At least 13 samples were used for real-time PCR analysis. **F–I,** Correlation of expression of the proteinase genes in the superficial zone of OA cartilage. Correlation coefficients of expression among the genes are shown on a heat map (**F**), and relationships of expression between *MMP2* (matrix metalloproteinase 2) and *ADAMTS5* (a disintegrin-like and metalloproteinase with thrombospondin type 1 motif, 5 [aggrecanase 2]), between *MMP3* (matrix metalloproteinase 3) and *MMP13* (matrix metalloproteinase 13), and between *MMP11* (matrix metalloproteinase 11) and *MMP13* are shown on scattergrams (**G–I,** respectively). Results of 42 OA cartilage samples are shown. In **F,** red and green colors indicate positive and negative correlations, respectively. * = $P < 0.05$; ** = $P < 0.01$. See Figure 1 for other definitions.

genes). The genes encoding metalloproteinases that could promote cartilage degeneration were assigned to the third group. The results of the microarray analysis and real-time PCR were compared in those 3 groups, respectively.

For 13 cartilage matrix genes, the result of microarray analysis was generally well consistent with that of real-time PCR, confirming the validity of our microarray analysis (Figure 1). The following features were noticed with the expression of cartilage matrix genes in OA cartilage. First, except for chitinase 3–like 1 (*CHI3L1*) (Figure 1K), the expression of all cartilage matrix genes was enhanced in OA cartilage. Second, despite such increase in expression, the change of gene expression across the zones was similar between OA and control cartilage. In other words, within OA cartilage, the level of increase in expression was similar in all 3 zones. Third, however, the degree of increase in expression was considerably different among the genes. For example, while the expression of *LECT1* and tenascin C (*TNC*) was increased 40 times and 220 times, respectively, in OA cartilage (Figures 1H and M), the increase of chondroadherin (*CHAD*) expression was merely 2-fold (Figure 1G).

Expression of bone-related genes. For this group of genes, the results were also consistent between the microarray and real-time PCR analyses (Figures 2A–H). The genes in this group were further divided into 2 categories by the pattern of expression across the zones. The expression of collagen, type I, α2 (*COL1A2*), *POSTN*, and tetranectin (*TNA*) was most enhanced in the superficial zone of OA cartilage (Figures 2A–C). Meanwhile, the expression of *COL10A1*, *IBSP*, secreted protein, acidic, cysteine-rich (*SPARC*), *SPP1*, and *WNT5B* was highest in the deep zone (Figures 2D–H). Since the expression of those genes in the control cartilage was very low, their expression in the specific zones of OA cartilage indicated the phenotypic change of the chondrocytes at those sites.

With these genes, a large difference was observed in expression levels among OA cartilage samples. For example, the expression level of *COL10A1* in the deep zone differed more than 1×10^4–fold among samples. If the induction of such gene expression was in fact related to the phenotypic change of the cells, there should be some correlation in their expression. To examine this possibility, we evaluated the expression of those genes in the superficial or deep zone in a greater number of OA cartilage samples. Among the 3 genes expressed in the superficial zone, a positive correlation was observed between *COL1A2* and *POSTN* ($r = 0.464$, $P < 0.001$) and between *POSTN* and *TNA* ($r = 0.300$, $P = 0.036$) (Figures 2I and J). A significant correlation was also observed among the 5 genes expressed in the deep zone.

Except for correlations between *IBSP* and *SPARC* and between *IBSP* and *WNT5B*, the expression of those 5 genes was significantly correlated in any other possible combination (Figure 2K). In particular, a close correlation was found between *COL10A1* and *WNT5B* ($r = 0.559$, $P < 0.001$), between *COL10A1* and *SPP1* ($r = 0.863$, $P < 0.001$), and between *SPARC* and *WNT5B* ($r = 0.511$, $P < 0.001$) (Figures 2L–N). This result implies that the expression of those bone-related genes could be induced in association with the phenotypic shift of the chondrocytes in the superficial and deep zones, respectively.

Expression of metalloproteinase genes. We also performed real-time PCR analysis on the expression of 5 metalloproteinase genes. Again, for these genes, the result of real-time PCR was almost consistent with that of the microarray analysis (Figures 3A–E). Interestingly, the expression of 2 proteinase genes was either not altered (a disintegrin-like and metalloproteinase with thrombospondin type 1 motif, 5 [aggrecanase 2]; termed *ADAMTS5*) (Figure 3E) or rather reduced (matrix metalloproteinase 3 [*MMP3*]) (Figure 3B) in OA cartilage compared with control cartilage. The expression of the other 3 genes was increased in OA cartilage. In particular, the expression of matrix metalloproteinase 11 (*MMP11*) and *MMP13* was highly enhanced in OA cartilage and reached >40-fold that in control cartilage.

The expression of these 5 proteinase genes, including 2 genes whose expression was not enhanced in OA cartilage, was most enhanced in the superficial zone. We then investigated the relationship of their expression in that zone in an increased number of OA cartilage samples. The results indicated that the expression of all 5 proteinase genes was mutually correlated (Figure 3F). A close correlation was observed between *MMP2* and *ADAMTS5* ($r = 0.876$, $P < 0.001$), between *MMP3* and *MMP13* ($r = 0.548$, $P < 0.001$), and between *MMP11* and *MMP13* ($r = 0.787$, $P < 0.001$) (Figures 3G–I), while a significant correlation was also seen between *MMP2* and *MMP11* ($r = 0.373$, $P = 0.009$) and between *MMP2* and *MMP13* ($r = 0.329$, $P = 0.023$).

DISCUSSION

In this study, the result of microarray analysis was in good agreement with that of real-time PCR (Figures 1–3) (see Supplementary Figure 1, available in the online version of this article at http://www3.interscience.wiley.com/journal/76509746/home). This corroborates the validity of our current analyses. Although some discrepancies were observed, they might not have been related to possible technical problems but more likely stemmed from individual differences in expression levels, given that a large individual difference is an inevitable problem in the analysis of human cartilage samples (2,20,21).

Our microarray analysis showed that ~40% of the investigated genes were expressed at significantly different levels among the zones. This zonal variation in expression would reflect both the physiologic difference in cell metabolism among the zones and the changes caused by the disease. This was illustrated by the expression of cartilage matrix genes (Figure 1). Our current analyses indicated that more than a dozen cartilage matrix genes were expressed at significantly different levels among the zones within OA cartilage. Despite this difference in gene expression levels, a similar zonal change of expression was observed in the control cartilage. Thus, it was assumed that in OA cartilage, the expression of those genes was amplified (or reduced) equally across the 3 zones by a certain mechanism(s) involved in the disease. This finding could be a clue for elucidating the mechanism(s) for enhanced matrix synthesis in OA, which remains entirely unknown.

Current analysis also revealed that the magnitude of the increase in expression was considerably different among the cartilage matrix genes. This finding may imply an unrecognized but potentially important mechanism for the progression of OA. Our current and previous evaluations showed that the 3 constitutive collagens of cartilage matrix (types II, IX, and XI collagen) could be synthesized at an altered ratio by OA chondrocytes (22). While the expression of *COL2A1* in OA cartilage was increased 10–24-fold that in control cartilage, the expression of collagen, type IX, α2 gene (*COL9A2*) and collagen, type XI, α1 gene (*COL11A1*) was enhanced 7–11-fold and 2–4-fold, respectively. In accordance with this, our analysis of cartilage collagens revealed that the amounts of pepsin-extractable type IX and type XI collagens are in fact reduced in OA cartilage relative to that of type II collagen (Fukui N: unpublished observations).

Type IX and type XI collagens form a collagen fibril network within cartilage, together with type II collagen. As known from observations of human hereditary diseases and gene-manipulated mice, the proper level of expression of these minor collagens is indispensable to maintain the normal properties of cartilage matrix (23–27). Therefore, the relative reduction of *COL9A2* and *COL11A1* expression in OA cartilage may lead to the fragility of newly synthesized cartilage, which might rather facilitate loss of cartilage matrix. Although

not yet demonstrated, disproportionate expression of other matrix components could have a similar significance in disease progression (28). We now assume that such imbalance in cartilage matrix gene expression could be significantly involved in the pathology of OA.

The expression of a series of bone-related genes in OA cartilage is another novel finding of this study. While the induction of *COL1A2* and *COL10A1* expression in OA cartilage has been known for more than a decade (2–4,21,29–36), enhanced expression of *TNA*, *POSTN*, *IBSP*, and *WNT5B* in human OA cartilage has not been reported previously. Our results suggested that the expression of these genes in OA cartilage could be related to the phenotypic change of the chondrocytes. The fact that their expression was induced either in the superficial zone or in the deep zone, and not in both, may reflect the occurrence of distinctive phenotypic changes in those zones.

Three among these bone-related genes expressed in the superficial zone (*COL1A2*, *POSTN*, and *TNA*) are known to be expressed by the osteoblasts (37,38). Meanwhile, 2 genes expressed in the deep zone (*COL10A1* and *WNT5B*) are expressed characteristically in the chondrocytes undergoing hypertrophic change (39). Thus, the phenotypic change in the superficial zone might have an aspect of osteoblastic differentiation, whereas that in the deep zone could have a trait of chondrocyte hypertrophy. In light of the developmental process of articular cartilage, this notion might not be unreasonable. At present, it is not known why these genes are expressed in OA cartilage. In the future, a more comprehensive analysis of gene expression profiles in the respective zones may clarify the molecular mechanism(s) involved in the phenotypic changes.

Meanwhile, the expression of 5 proteinase genes was most enhanced in the superficial zone of OA cartilage. In OA, the cartilage surface is the region where cartilage degeneration begins (10–12). Therefore, those proteinases could be responsible for the initiation of matrix degeneration at that site. Furthermore, the finding that their expression was mutually correlated at the superficial zone implies that those proteinases could work synergistically in certain cases to cause cartilage degeneration. That correlation also suggests the presence of a common regulatory mechanism(s) for their expression. Regulation of proteinase expression in OA cartilage is critically important to inhibit the progression of the disease. Thus, elucidation of such a mechanism(s) may be useful to develop new therapeutic strategies for OA.

Although it is important, the change of chondrocyte metabolism in OA has been understood only partly. This incomplete understanding could be ascribed, at least in part, to the regional difference in cellular metabolism within cartilage. As demonstrated in this study, consideration of the regional difference within cartilage could provide further insights into the metabolic change of the chondrocytes with the disease. Conventionally, such regional differences have been studied by histologic evaluations of a limited number of genes. Compared with those techniques, the experimental methods we employed here could be advantageous in that they allow a more comprehensive evaluation of the cellular metabolism in specific sites. Obviously, this study has several limitations. The number of samples used for the microarray analysis was rather small, and the number of genes contained in the array was limited to 527. Although confirmed for selected genes, the reliability of the microarray analysis has not been fully validated. Therefore, it is very likely that some genes are left unnoticed while they are expressed at different intensities across the zones. For all its limitations, the present study promises to provide greater understanding of the pathology of OA.

AUTHOR CONTRIBUTIONS

Drs. Fukui and Ikegawa had full access to all of the data in the study and take responsibility for the integrity of the data and the accuracy of the data analysis.

Study design. Fukui, Ikegawa.

Acquisition of data. Miyamoto, Nakajima, Ikeda, Hikita, Furukawa, Mitomi, Tanaka, Katsuragawa, Yamamoto, Sawabe, Juji, Mori, Suzuki.

Analysis and interpretation of data. Fukui, Miyamoto, Nakajima.

Manuscript preparation. Fukui, Ikegawa.

Statistical analysis. Fukui, Miyamoto, Nakajima.

REFERENCES

1. Pelletier JP, Martel-Pelletier J, Abramson SB. Osteoarthritis, an inflammatory disease: potential implication for the selection of new therapeutic targets. Arthritis Rheum 2001;44:1237–47.
2. Fukui N, Ikeda Y, Ohnuki T, Tanaka N, Hikita A, Mitomi H, et al. Regional differences in chondrocyte metabolism in osteoarthritis: a detailed analysis by laser capture microdissection. Arthritis Rheum 2008;58:154–63.
3. Von der Mark K, Kirsch T, Nerlich A, Kuss A, Weseloh G, Gluckert K, et al. Type X collagen synthesis in human osteoarthritic cartilage: indication of chondrocyte hypertrophy. Arthritis Rheum 1992;35:806–11.
4. Aigner T, Bertling W, Stoss H, Weseloh G, von der Mark K. Independent expression of fibril-forming collagens I, II, and III in chondrocytes of human osteoarthritic cartilage. J Clin Invest 1993;91:829–37.
5. Young RD, Lawrence PA, Duance VC, Aigner T, Monaghan P. Immunolocalization of collagen types II and III in single fibrils of human articular cartilage. J Histochem Cytochem 2000;48:423–32.
6. Buckwalter JA, Mankin HJ, Grodzinsky AJ. Articular cartilage

and osteoarthritis. In: Pellegrini VD Jr, editor. AAOS instructional course lectures. Vol 54. Rosemont (IL): American Academy of Orthopaedic Surgeons; 2005. p. 465–80.
7. Poole RA. Cartilage in health and disease. In: Koopman WJ, Moreland LW, editors. Arthritis and allied conditions: a textbook of rheumatology. 15th ed. Philadelphia: Lippincott Williams & Wilkins; 2004. p. 223–69.
8. Sandell LJ, Heinegard D, Hering TM. Cell biology, biochemistry, and molecular biology of articular cartilage in osteoarthritis. In: Moskowitz RW, Altman RD, Hochberg MC, Buckwalter JA, Goldberg VM, editors. Osteoarthritis: diagnosis and medical/surgical management. 4th ed. Philadelphia: Lippincott Williams & Wilkins; 2007. p. 73–106.
9. Mow VC, Hung CT. Mechanical properties of normal and osteoarthritic articular cartilage, and the mechanobiology of chondrocytes. New York: Oxford University Press; 2003.
10. Hollander AP, Pidoux I, Reiner A, Rorabeck C, Bourne R, Poole AR. Damage to type II collagen in aging and osteoarthritis starts at the articular surface, originates around chondrocytes, and extends into the cartilage with progressive degeneration. J Clin Invest 1995;96:2859–69.
11. Lark MW, Bayne EK, Flanagan J, Harper CF, Hoerrner LA, Hutchinson NI, et al. Aggrecan degradation in human cartilage: evidence for both matrix metalloproteinase and aggrecanase activity in normal, osteoarthritic, and rheumatoid joints. J Clin Invest 1997;100:93–106.
12. Poole RA, Guilak F, Abramson SB. Etiopathogenesis of osteoarthritis. In: Moskowitz RW, Altman RD, Hochberg MC, Buckwalter JA, Goldberg VM, editors. Osteoarthritis: diagnosis and medical/surgical management. 4th ed. Philadelphia: Lippincott Williams & Wilkins; 2007. p. 27–49.
13. Emmert-Buck MR, Bonner RF, Smith PD, Chuaqui RF, Zhuang Z, Goldstein SR, et al. Laser capture microdissection. Science 1996;274:998–1001.
14. Altman R, Asch E, Bloch D, Bole G, Borenstein D, Brandt K, et al. Development of criteria for the classification and reporting of osteoarthritis: classification of osteoarthritis of the knee. Arthritis Rheum 1986;29:1039–49.
15. Baelde HJ, Cleton-Jansen AM, van Beerendonk H, Namba M, Bovee JV, Hogendoorn PC. High quality RNA isolation from tumours with low cellularity and high extracellular matrix component for cDNA microarrays: application to chondrosarcoma. J Clin Pathol 2001;54:778–82.
16. Zhang H, Liew CC, Marshall KW. Microarray analysis reveals the involvement of β-2 microglobulin (B2M) in human osteoarthritis. Osteoarthritis Cartilage 2002;10:950–60.
17. Zhang H, Marshall KW, Tang H, Hwang DM, Lee M, Liew CC. Profiling genes expressed in human fetal cartilage using 13,155 expressed sequence tags. Osteoarthritis Cartilage 2003;11:309–19.
18. Matsumura H, Bin Nasir KH, Yoshida K, Ito A, Kahl G, Kruger DH, et al. SuperSAGE array: the direct use of 26-base-pair transcript tags in oligonucleotide arrays. Nat Methods 2006;3: 469–74.
19. Nuwaysir EF, Huang W, Albert TJ, Singh J, Nuwaysir K, Pitas A, et al. Gene expression analysis using oligonucleotide arrays produced by maskless photolithography. Genome Res 2002;12: 1749–55.
20. Yagi R, McBurney D, Laverty D, Weiner S, Horton WE Jr. Intrajoint comparisons of gene expression patterns in human osteoarthritis suggest a change in chondrocyte phenotype. J Orthop Res 2005;23:1128–38.
21. Aigner T, Fundel K, Saas J, Gebhard PM, Haag J, Weiss T, et al. Large-scale gene expression profiling reveals major pathogenetic pathways of cartilage degeneration in osteoarthritis. Arthritis Rheum 2006;54:3533–44.
22. Fukui N, Ikeda Y, Ohnuki T, Yamane S, Suzuki R, Yamamoto S, et al. Integrin $\alpha5\beta1$ may be responsible for the induction of type I and type III collagen during dedifferentiation in the monolayer cultured adult human articular chondrocytes. Osteoarthritis Cartilage 2005;13 Suppl A:S20–1.
23. Briggs MD, Chapman KL. Pseudoachondroplasia and multiple epiphyseal dysplasia: mutation review, molecular interactions, and genotype to phenotype correlations. Hum Mutat 2002;19:465–78.
24. Fassler R, Schnegelsberg PN, Dausman J, Shinya T, Muragaki Y, McCarthy MT, et al. Mice lacking $\alpha1$(IX) collagen develop noninflammatory degenerative joint disease. Proc Natl Acad Sci U S A 1994;91:5070–4.
25. Hu K, Xu L, Cao L, Flahiff CM, Brussiau J, Ho K, et al. Pathogenesis of osteoarthritis-like changes in the joints of mice deficient in type IX collagen. Arthritis Rheum 2006;54:2891–900.
26. Spranger J. The type XI collagenopathies. Pediatr Radiol 1998; 28:745–50.
27. Xu L, Flahiff CM, Waldman BA, Wu D, Olsen BR, Setton LA, et al. Osteoarthritis-like changes and decreased mechanical function of articular cartilage in the joints of mice with the chondrodysplasia gene (cho). Arthritis Rheum 2003;48:2509–18.
28. Cs-Szabo G, Melching LI, Roughley PJ, Glant TT. Changes in messenger RNA and protein levels of proteoglycans and link protein in human osteoarthritic cartilage samples. Arthritis Rheum 1997;40:1037–45.
29. Girkontaite I, Frischholz S, Lammi P, Wagner K, Swoboda B, Aigner T, et al. Immunolocalization of type X collagen in normal fetal and adult osteoarthritic cartilage with monoclonal antibodies. Matrix Biol 1996;15:231–8.
30. Boos N, Nerlich AG, Wiest I, von der Mark K, Ganz R, Aebi M. Immunohistochemical analysis of type-X-collagen expression in osteoarthritis of the hip joint. J Orthop Res 1999;17:495–502.
31. Adam M, Deyl Z. Altered expression of collagen phenotype in osteoarthrosis. Clin Chim Acta 1983;133:25–32.
32. Aigner T, Gluckert K, von der Mark K. Activation of fibrillar collagen synthesis and phenotypic modulation of chondrocytes in early human osteoarthritic cartilage lesions. Osteoarthritis Cartilage 1997;5:183–9.
33. Aigner T, Reichenberger E, Bertling W, Kirsch T, Stoss H, von der Mark K. Type X collagen expression in osteoarthritic and rheumatoid articular cartilage. Virchows Arch B Cell Pathol Incl Mol Pathol 1993;63:205–11.
34. Aigner T, Zien A, Gehrsitz A, Gebhard PM, McKenna L. Anabolic and catabolic gene expression pattern analysis in normal versus osteoarthritic cartilage using complementary DNA-array technology. Arthritis Rheum 2001;44:2777–89.
35. Goldwasser M, Astley T, van der Rest M, Glorieux FH. Analysis of the type of collagen present in osteoarthritic human cartilage. Clin Orthop Relat Res 1982;(167):296–302.
36. Miosge N, Hartmann M, Maelicke C, Herken R. Expression of collagen type I and type II in consecutive stages of human osteoarthritis. Histochem Cell Biol 2004;122:229–36.
37. Wewer UM, Ibaraki K, Schjorring P, Durkin ME, Young MF, Albrechtsen R. A potential role for tetranectin in mineralization during osteogenesis. J Cell Biol 1994;127:1767–75.
38. Horiuchi K, Amizuka N, Takeshita S, Takamatsu H, Katsuura M, Ozawa H, et al. Identification and characterization of a novel protein, periostin, with restricted expression to periosteum and periodontal ligament and increased expression by transforming growth factor β. J Bone Miner Res 1999;14:1239–49.
39. Church V, Nohno T, Linker C, Marcelle C, Francis-West P. Wnt regulation of chondrocyte differentiation. J Cell Sci 2002;115: 4809–18.

Inhibition of Src Homology 2 Domain-Containing Protein Tyrosine Phosphatase Substrate-1 Reduces the Severity of Collagen-Induced Arthritis

KONAGI TANAKA, TATSUYA HORIKAWA, SATSUKI SUZUKI, KAZUTAKA KITAURA, JUNKO WATANABE, AKITO GOTOH, NORIYUKI SHIOBARA, TSUNETOSHI ITOH, SHOJI YAMANE, RYUJI SUZUKI, NAOSHI FUKUI, and TAKAHIRO OCHI

Reprinted from the JOURNAL OF RHEUMATOLOGY

Volume 35, Number 12, December 2008

Pages 2316-2324